1521-009X/50/7/1027–1041$35.00
DRUG METABOLISM AND DISPOSITION
dx.doi.org/10.1124/dmd.121.000478
Drug Metab Dispos 50:1027–1041, July 2022

Special Section on Drug Metabolism and Regulation—Minireview

From Steroid and Drug Metabolism to Glycobiology, Using Sulfotransferase Structures to Understand and Tailor Function

Lars C. Pedersen, MyeongJin Yi, Lee G. Pedersen, and Andrea M. Kaminski

Genome Integrity and Structural Biology Laboratory (L.C.P., L.G.P., A.M.K.) and Reproductive and Developmental Biology Laboratory (M.Y.), National Institute of Environmental Health Sciences, National Institutes of Health, Research Triangle Park, North Carolina; and Department of Chemistry, University of North Carolina at Chapel Hill, Chapel Hill, North Carolina (L.G.P.)

Received March 22, 2021; accepted December 6, 2021

ABSTRACT

Sulfotransferases are ubiquitous enzymes that transfer a sulfo group from the universal cofactor donor 3′-phosphoadenosine 5′-phosphosulfate to a broad range of acceptor substrates. In humans, the cytosolic sulfotransferases are involved in the sulfation of endogenous compounds such as steroids, neurotransmitters, hormones, and bile acids as well as xenobiotics including drugs, toxins, and environmental chemicals. The Golgi associated membrane-bound sulfotransferases are involved in post-translational modification of macromolecules from glycosaminoglycans to proteins. The sulfation of small molecules can have profound biologic effects on the functionality of the acceptor, including activation, deactivation, or enhanced metabolism and elimination. Sulfation of macromolecules has been shown to regulate a number of physiologic and pathophysiological pathways by enhancing binding affinity to regulatory proteins or binding partners. Over the last 25 years, crystal structures of these enzymes have provided a wealth of information on the mechanisms of this process and the specificity of these enzymes. This review will focus on the general commonalities of the sulfotransferases, from enzyme structure to catalytic mechanism as well as providing examples into how structural information is being used to either design drugs that inhibit sulfotransferases or to modify the enzymes to improve drug synthesis.

SIGNIFICANCE STATEMENT

This manuscript honors Dr. Masahiko Negishi's contribution to the understanding of sulfotransferase mechanism, specificity, and roles in biology by analyzing the crystal structures that have been solved over the last 25 years.

Introduction

The sulfated products of reactions catalyzed by the sulfotransferase family of enzymes are involved in many physiologic and pathophysiological processes (Gamage et al., 2006; Bishop et al., 2007; Duffel, 2010 updated 2016; Lindahl et al., 2015; Coughtrie, 2016; Langford et al., 2017). Vertebrate sulfotransferases use 3′-phosphoadenosine 5′-phosphosulfate (PAPS) as the universal sulfo donor. PAPS is synthesized by one of two PAPS synthases, which are bifunctional enzymes that use two ATP molecules to produce one molecule of PAPS (Fig. 1) (Lyle et al., 1994; Xu et al., 2000). The ATP sulfurylase domain displaces pyrophosphate from ATP with inorganic sulfate to produce adenosine 5′-phosphosulfate (APS). APS is subsequently phosphorylated at the 3′ hydroxyl by the APS kinase domain to produce PAPS.

Sulfation by cytosolic sulfotransferases (SULTs) of small molecules on hydroxyl or amine moieties is one of the major pathways for the detoxification of xenobiotics and elimination of endogenous small molecules such as hormones, neurotransmitters, and bile acids from the body (Gamage et al., 2006; Duffel, 2010 updated 2016; Coughtrie, 2016). Sulfation of these compounds typically improves water solubility, enhancing elimination. However, sulfation can also result in biologically active compounds. Dehydroepiandrosterone and estrone sulfate can act as circulating intermediates for the biosynthesis of hormones, whereas pregnenolone sulfate can regulate neurotransmitter receptors (Mueller et al., 2015). As such, sulfation/desulfation is a critical process that modulates steroidogenesis and hormone action in various tissues (Mueller et al., 2015). Inhibition of sulfotransferases due to environmental exposures to chemicals such as polychlorinated biphenols and flame retardants may result in disruption of proper endocrine homeostasis (Kester et al., 2000, 2002; Hamers et al., 2008).

In addition to aiding in the elimination of dietary compounds and environmental toxins, SULTs are major Phase II drug metabolizing enzymes, not only involved in their elimination, but also in the activation of prodrugs. Sulfation of minoxidil, for example, is critical for its hair growth effects, whereas sulfation of oxamniquine activates the drug to treat schistosomiasis (Buhl et al., 1990; Pica-Mattoccia et al., 2006; Valentim et al., 2013).

This work was supported by the Division of Intramural Research of the National Institutes of Health, National Institutes of Environmental Health Sciences [Grant 1ZIA-ES102645] (to L.C.P).
dx.doi.org/10.1124/dmd.121.000478.

ABBREVIATIONS: APS, adenosine 5′-phosphosulfate; GAG, glycosaminoglycan; GlcA, glucuronic acid; GlcNAc, N-acetylglucosamine; HSST, heparan sulfate sulfotransferase; IdoA, Iduronic acid; MD, molecular dynamics; NDST-1, N-deacetylase/N-sulfotransferase isoform 1; NST-1, sulfotransferase domain of NDST-1; OST, O-sulfotransferase; PAP, 3′-phosphoadenosine 5′-phosphate; PAPS, 3′-phosphoadenosine 5′-phosphosulfate; PDB, protein data bank; PSB, phosphosulfate binding; SB, sulfate binding; SULT, cytosolic sulfotransferase; TPST, Tyrosyl protein sulfotransferase.

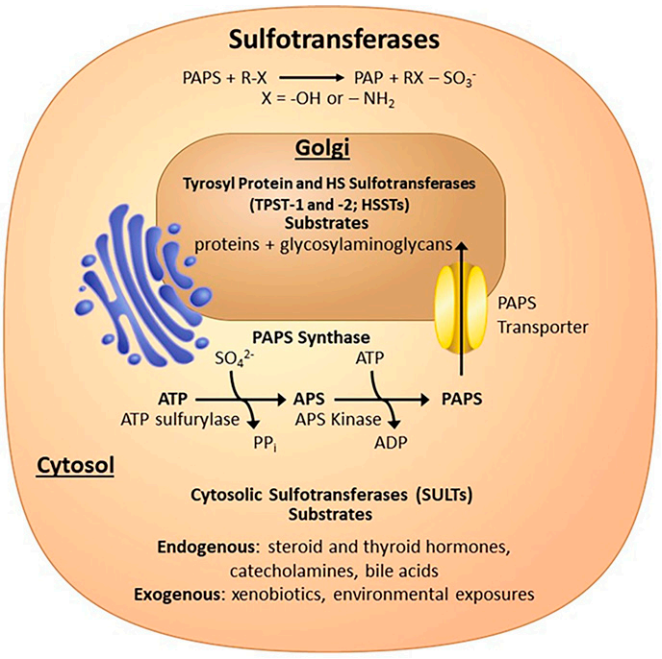

Fig. 1. Sulfotransferases covered in this review. Sulfotransferases transfer a sulfo group (SO_3) from PAPS, which is generated in the cytosol by the bifunctional PAPS synthases to many different types of acceptor substrates. The SULT enzymes in the cytosol sulfate endogenous and exogenous small molecules, whereas the Golgi-associated sulfotransferase sulfate macromolecules such as proteins and glycosaminoglycans.

In humans, there are 13 SULT genes encoding 14 proteins, with two of the proteins resulting from alternative splicing (Coughtrie, 2016). These proteins are between 284 to 365 amino acids in length. Historical nomenclature for the SULTs was based upon the original substrate with which they were identified (e.g., EST estrogen sulfotransferase, PST phenol sulfotransferase, and AST aryl sulfotransferase), but as it became clear that many of these enzymes catalyzed substrates with different functional groups and exhibited overlapping specificity, a more systematic nomenclature was needed (Blanchard et al., 2004; Duffel, 2010 updated 2016). In brief, in the current nomenclature, the first numeral after the SULT defines the family (45% sequence identity) and the following capital Arabic letter defines the subfamily (60%), with the final numeral defining the isoform. Splice variants are then assigned a lowercase letter (ex. SULT2B1b).

Tyrosyl protein sulfotransferases (TPSTs) are Type-II integral membrane proteins localized in the *trans*-Golgi network that are responsible for sulfation of the tyrosine side chain of acceptor proteins, representing one of the major post-translational modifications (Fig. 1) (Moore, 2003). Tyrosine sulfation can have a number of biologic consequences including effecting circulation half-life, proteolytic processing of bioactive peptides, and protein-protein interactions impacting many processes including blood coagulation, inflammation, and viral infection (Leyte et al., 1991; Pouyani and Seed, 1995; Farzan et al., 1999; Moore, 2003). Humans contain two TPSTs (TPST-1 and -2) that share 64% sequence identity and are 370 and 377 amino acids in length, respectively (Niehrs and Huttner, 1990; Beisswanger et al., 1998; Ouyang et al., 1998). These enzymes have broad and slightly different substrate specificities (Mishiro et al., 2006).

There are at least 37 Golgi-associated sulfotransferases in humans, a large number of which are involved in the sulfation of the glycosaminoglycans (GAGs)—heparan sulfate, chondroitin sulfate, and dermatan sulfate (Langford et al., 2017; Zerbino et al., 2018). These GAGs are found attached to a select group of specific proteins or lipids and are found ubiquitously on the cell surface and in the extracellular matrix (Bishop et al., 2007; Lindahl and Li, 2009; Iozzo and Schaefer, 2015; Lindahl et al., 2015). As such, they play important roles in how cells communicate with their surrounding environment through interactions with protein binding partners. These GAGs are involved in a long list of physiologic and pathophysiological processes including embryonic development, blood coagulation, inflammation, bacterial and viral infection, neurodegenerative diseases, and cancer (Bishop et al., 2007; Lindahl and Li, 2009; Shi et al., 2021). GAGs are made up of linear repeating disaccharide units that can be modified by deacetylation, epimerization, and sulfation. This review will focus on heparan sulfate sulfotransferases due to the availability of structural information. The sulfation of specific hydroxyls and amines on the GAGs is carried out by unique sulfotransferases and appears to be a somewhat ordered process (Multhaupt and Couchman, 2012). In general, heparan sulfates (HS) are synthesized through chain elongation by a set of glycosyltransferases (exotosin 1 and 2) onto a common linker region to produce repeating disaccharides units of *N*-acetylglucosamine (GlcNAc) and glucuronic acid (GlcA). The bifunctional *N*-deacetylase/N-sulfotransferase (4 isoforms in humans) can deacetylate and subsequently sulfate the glucosamine at the 2-amine position. This becomes a good substrate for the C_5-epimerase, which can convert adjacent GlcAs into iduronic acids (IdoA). Although the 2-*O*-sulfotranerase (1 isoform) can sulfate the 2-hydroxyl on GlcA, sulfation on IdoA appears to be the preferred substrate and is much more prevalent in biology (Rong et al., 2001; Bethea et al., 2008; Liu et al., 2014). Sulfation by both the 6-*O*-sulfotransferases (3 isoforms) and the 3-*O*-sulfotransfereases (7 isoforms) occurs at the 6- and 3-hydroxyl groups of glucosamines, respectively. Whereas some sulfotransferase isoforms appear to have similar substrate specificities, others are very distinct. The extent and types of modification in a given tissue or cell type are spatially and temporally regulated and are determined by which isoforms are present and expressed.

Historical Prospective

In 1876, the relevance of sulfotransferases in medicine was first reported when E. Baumann determined that the conjugate of carbolic acid, a common antiseptic used in surgery at the time, could be absorbed by the skin and secreted in the urine as phenol sulphuric ester (Baumann, 1876; Folin and Denis, 1915). Recognizing the importance and relevance of sulfation in chondroitin sulfate, heparin, steroids, and phenol detoxification, Robbins and Lipmann reported in 1956 that the biologic sulfo donor was indeed PAPS, which could be produced by a liver enzyme with the addition of ATP (Robbins and Lipmann, 1956; Lipmann, 1958). They referred to the enzymes that must use PAPS for the sulfo donor as sulfokinases. It was around this same time period that the first tyrosine-*O*-sulfate was found in a peptide from fibrinogen (Bettelheim, 1954). By this time, HS had already been identified as an effective anticoagulant and had been introduced as a widely available therapeutic (Howell and Holt, 1918; Lim, 2017). It wasn't until 1987 that the first cytosolic sulfotransferase was unknowingly cloned as an androgen-repressible rat liver protein (Chatterjee et al., 1987). The cloning of the first Golgi sulfotransferases involved in HS biosynthesis occurred in 1992, and the TPSTs followed in 1998 (Hashimoto et al., 1992; Ouyang et al., 1998).

Prior to the first crystal structures, sequence alignments of the SULTs were used to identify critical residues in the functionality of these enzymes (Roche et al., 1991; Khan et al., 1993; Weinshilboum and Otterness, 1994). These alignments revealed two highly conserved regions including an N-terminal region YPKSGTXW and a carboxy terminus GXXGXXK reminiscent of the GXXXXGK[TS] P-loop structures found to bind ATP in kinases (Saraste et al., 1990). In 1997, the

Negishi laboratory at the National Institute of Environmental Health Sciences at the National Institutes of Health published the first crystal structure of a sulfotransferase (mouse estrogen sulfotransferase or mSULT1E1), ushering in a new era of understanding of the molecular function of these enzymes (Kakuta et al., 1997). This structure revealed that both regions indeed bound to the PAPS; however, it was the amino terminal region that was structurally related to the P-loop and cradled the 5′-phosphate, whereas the C-terminal region bound to the 3′-phosphate unique to PAPS (Fig. 2). The structure also revealed a conservation of a central scaffold as well as substrate positioning similar to that of the adenylate kinase family of enzymes, suggesting a common mechanism between sulfation and phosphorylation. This analogy can be extended to desulfation, since sulfatases display conservation in structure and activity to that of alkaline phosphatase (Bond et al., 1997; O'Brien and Herschlag, 1998). Crystal structures currently exist for 12 of the 14 human SULTs, representatives from each of the vertebrate HS sulfotransferases as well as both TPSTs (Table 1).

In this review, we will delve into what has been learned from crystal structures of the various sulfotransferase families (SULTs, HSSTs, and TPSTs) regarding conservation of structure and mechanism, determinants of specificity, and how this information is being used to design and engineer new pharmacological tools.

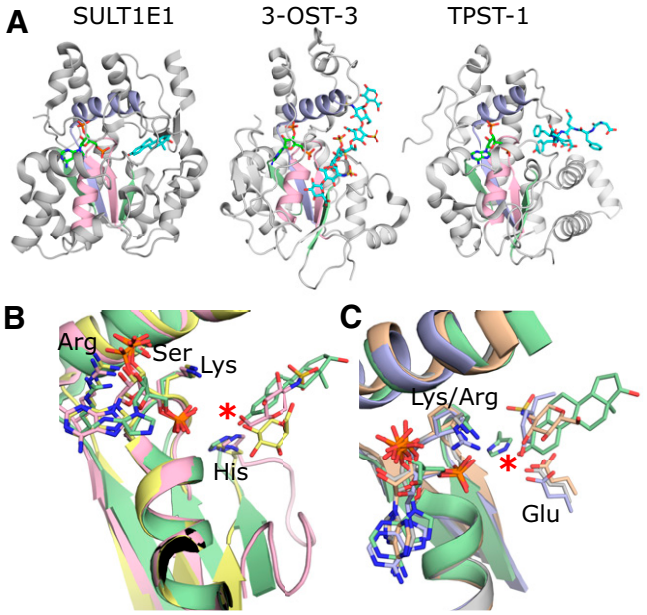

Fig. 2. Representative structures of the different types of sulfotransferases and their PAPS binding sites. (A) From left to right: crystal structure of hSULT1E1 in complex with PAP and estradiol [protein data bank (PDB) code 4JVL) (Gosavi et al., 2013); crystal structure of 3-OST-3 with PAP and an 8mer NS2S heparan sulfate bound (PDB code 6XL8) (Wander et al., 2021); crystal structure of TPST-1 with PAP and a polypeptide substrate bound (PDB code 5WRI) (Tanaka et al., 2017). The PAP is colored green and acceptor substrates are cyan. The strand-loop-helix containing the PSB loop is colored pink, whereas the strand-loop-helix containing the 3′-phosphate binding motif (3′SB) is colored light purple. The remaining two strands making up the central β-sheet are colored light green. (B) Comparisons of the PAP binding motifs and catalytic residues. The SULTs including SULT1E1 (green) and heparan sulfotransferases 2-OST (yellow) and 6-OST (pink) all use a lysine on the PSB loop and histidines for the proposed catalytic base (PDB codes 4JVL, 4NDZ, and 5T0A, respectively) (Gosavi et al., 2013; Liu et al., 2014; Xu et al., 2017b). The acceptor hydroxyl on the substrates all superimpose well, supporting a conserved mechanism. (C) Comparisons of the PAP binding motifs and catalytic residues of the sulfotransferase domain of SULT1E1 (green), NDST-1 (gray), 3-OST-3 (wheat), and TPST-1 (light purple) (PDB codes: 4JVL, NST1, 6XL8, and 5WRI, respectively) (Kakuta et al., 1999; Gosavi et al., 2013; Tanaka et al., 2017; Wander et al., 2021). NDST-1, 3-OST-3, and TPST-1 appear to use a conserved glutamate for their catalytic base, as opposed to the SULTs, 2-OST, and 6-OST. However, the PAPs and acceptor hydroxyls on the substrates all superimpose perfectly, supporting a conserved inline reaction mechanism for all the vertebrate sulfotransferases. For panels B and C, only the acceptor saccharide of the substrate is shown for 3-OST-3 and 2-OST and acceptor tyrosine of the peptide for TPST-1. No substrate is present in the crystal structure of NST-1.

Key Advances in Understanding

Conservation of Structure and Mechanism among Sulfotransferases. The crystal structures of SULTs, heparan sulfate sulfotransferases (HSSTs), and TPSTs all share many central commonalities with respect to structure and function. All three families of sulfotransferases contain a conserved core structure consisting of 4–5 β-strands flanked on both faces with α-helixes (Fig. 2A) (Negishi et al., 2001; Teramoto et al., 2013; Gunal et al., 2019). The need for binding specificity to PAPS dictates structural conservation throughout the sulfotransferases. From the structural analysis of mouse estrogen sulfotransferase (mSULT1E1), two conserved motifs were identified (Fig. 2) (Kakuta et al., 1997). The first strand-loop-helix motif is analogous to the P-loop structures found in the uridylate kinase family that cradles the 5′-phosphate of the PAPS, forming an extensive hydrogen bonding network via backbone amide interactions with the loop [referred to as the termed phosphosulfate binding (PSB)-loop] (Kakuta et al., 1998a). Central to the loop is a conserved basic residue, usually a lysine but sometimes an arginine (such as in the TPSTs) that hydrogen bonds to the 5′-phosphate (Fig. 2, B–C) (Teramoto et al., 2013; Valentim et al., 2013). The second region, termed 3′-sulfate binding (SB), consists of a strand from the central β-sheet and an α-helix that runs across the top of the PSB loop that can form interactions with both the donor and acceptor substrates (Fig. 2) (Kakuta et al., 1998a). This region is involved in binding of the 3′-phosphate of the 3′-phosphoadenosine 5′-phosphate (PAP) via sidechain interactions with a conserved arginine from the β-strand and a serine residue from the 3′SB α-helix (Fig. 2, B–C). The SULTs contain an additional conserved region of sequence GXXGXXK that, as mentioned, was proposed to interact with the PAPS based on its similarity in sequence to P-loops (Marsolais and Varin, 1995). The structure of mSULT1E1 revealed that indeed this region interacted with the PAPS, but via the 3′-phosphate, and perhaps plays other critical roles in function, as discussed later.

The relative position of the substrate acceptor with respect to the position of the donor suggested an inline displacement mechanism for the sulfo group transfer (Fig. 3, A–C) (Kakuta et al., 1997). This was further supported by a cocrystal structure of mSULT1E1 with vanadate and estradiol, as well as mSULT1E1 with PAPS alone (Fig. 3D) (Kakuta et al., 1998b; Pedersen et al., 2002). Based on the structural comparisons to uridylate kinase, it was hypothesized that the reaction would proceed via an S_N2-like associative reaction mechanism whereby the acceptor nucleophile could be primed by a catalytic base, allowing for nucleophilic attack on the sulfur of PAPS (Müller-Dieckmann and Schulz, 1994; Kakuta et al., 1997). The reaction would proceed through a trigonal bipyramidal transition state, with the leaving oxygen on the PAP and the incoming nucleophile in the axial positions (Fig. 3B). This transition state was proposed to be mimicked by the crystal structure of mSULT1E1 in the presence of PAP and vanadate (Fig. 3D) (Kakuta et al., 1998b). In the mSULT1E1/PAPS structure, the position of the conserved lysine on the PSB loop is found in a different orientation than when PAP is bound (Fig. 3D) (Pedersen et al., 2002). Here, the lysine is found hydrogen bonding with the conserved serine from the 3′SB loop rather than with the 5′-phosphate of the PAP. It was proposed that this interaction discourages PAPS hydrolysis in the absence of

TABLE 1

Representative structures of the human SULT, TPST, and HSSTs

Sulfotransferase	Acceptor	Nucleotide	PDB Code	Res Å	Reference
Human Cytosolic Sulfotransferases (SULTs)					
SULT1A1	p-nitrophenol	PAP	1LS6	1.9	(Gamage et al., 2003)
	estradiol	PAP	2D06	2.3	(Gamage et al., 2005)
	p-nitrophenol	PAP	3QVU	2.5	(Alcolombri et al., 2011)
	3-cyanoumbelliferone	PAP	3QVV	2.35	(Alcolombri et al., 2011)
	2-napthol	PAP	3U3K	2.36	(Berger et al., 2011)
	3-cyano-7-hydroxycoumarin	PAP	3U3M, 3U3O	2.3, 2.0	(Berger et al., 2011)
	p-nitrophenol	PAP	3U3R	2.36	(Berger et al., 2011)
	—	PAP	3U3J	2.70	(Berger et al., 2011)
	—	PAP	4GRA	2.56	(Cook et al., 2013a)
SULT1A1*3	—	PAP	1Z28	2.3	(Lu et al., 2010)
SULT1A2		PAP	1Z29	2.4	(Lu et al., 2010)
SULT1A3	Dopamine	PAP	2A3R	2.6	(Lu et al., 2005)
	—	—	1CJM	2.4	(Bidwell et al., 1999)
SULT1B1	Resveratrol	PAP	3CKL	2.0	TBP[f]
	—	PAP	2Z5F	2.1	(Dombrovski et al., 2006)
SULT1C2[a]	—	PAP	3BFX	1.8	(Dombrovski et al., 2006)
SULT1C3d	—	PAP	2H8K	3.2	(Allali-Hassani et al., 2007)
	—	PAP	2REO	2.65	TBP
SULT1C4[b]	Pentrachlorophenol	PAP	2GWH	1.80	(Allali-Hassani et al., 2007)
	—	—	2AD1	2.00	(Allali-Hassani et al., 2007)
SULT1E1	Estradiol	PAP	4JVL	1.94	(Gosavi et al., 2013)
	Tetrabromobisphenol A	PAP	4JVM	1.99	(Gosavi et al., 2013)
	3,5,3′,5′-tetrachloro-biphenyl-4-4’-diol	PAP	1G3M	1.7	(Shevtsov et al., 2003)
	3-hydroxylbromodiphenyl ether	PAP	4JVN	2.05	(Gosavi et al., 2013)
	—	PAPS	1HY3	1.80	(Pedersen et al., 2002)
SULT2A1	Androsterone	—	1OV4	2.70	(Chang et al., 2004)
	DHEA[g]	—	1J99	1.99	(Rehse et al., 2002)
	(3Beta,5alpha)-3-Hydroxyandrostan-17-one	—	2QP32QP4	2.6 3.0	(Lu et al., 2008)
	Lithocholic acid	PAP	3F3Y	2.2	TBP
		PAPS	4IFB	2.3	TBP
	—	PAP	1EFH	2.4	(Pedersen et al., 2000)
SULT2B1a	—	PAP	1Q1Q	2.91	(Lee et al., 2003)
SULT2B1b	DHEA	PAP	1Q22	2.5	(Lee et al., 2003)
	Pregnenolone	PAP	1Q20	2.3	(Lee et al., 2003)
	—	PAP	1Q1Z	2.4	(Lee et al., 2003)
SULT4A1	—	—	1ZD1	2.24	(Allali-Hassani et al., 2007)
Tyrosyl Protein Sulfotransferase (TPSTs)					
TPST-1	DFED**Y**EFD	PAP	5WRI	1.60	(Tanaka et al., 2017)
	EEEEEA**Y**GWMDF	PAP	5WRJ	2.33	(Tanaka et al., 2017)
TPST-2	EDFED**Y**EFD		3AP1	1.9	(Teramoto et al., 2013)
	EDFED**Y**EFD	PAP	3AP2	2.4	TBP
	—	PAP	3AP3	3.5	(Teramoto et al., 2013)
Heparan Sulfate Sulfotransferases (HSSTs)					
NDST-1 (sulfotransferase catalytic domain)	—	PAP	1NST		(Kakuta et al., 1999)
2-OST[c]	GlcA-GlcNAc-GlcA-GlcNS-**IdoA**[h]-GlcNS-GlcA-pNP	PAP	4NDZ	3.45	(Liu et al., 2014)
	—	PAP	3F5F	2.65	(Bethea et al., 2008)
6-OST-3[d]	**GlcNS**-GlcA-GlcNS-IdoA2S-GlcNS-GlcA-pNP	PAP	5T05	1.95	(Xu et al., 2017b)
	GlcNS-GlcA-GlcNS-GlcA-GlcNS-GlcA-pNP	PAP	5T03	2.1	(Xu et al., 2017b)
	GlcA-**GlcNS**-GlcA-GlcNS-GlcA-GlcNS-GlcA-pNP	PAP	5T0A	1.95	(Xu et al., 2017b)

TABLE 1 *continued*

Sulfotransferase	Acceptor	Nucleotide	PDB Code	Res Å	Reference
3-OST-1[e]	GlcNAc6S-GlcA-**GlcNS6S**-IdoA2S-GlcNS6S-GlcA-UA	PAP	3UAN	1.84	(Moon et al., 2012)
	—	PAP	1VKJ	2.5	(Edavettal et al., 2004)
3-OST-1	—	PAP	1ZRH	2.1	TBP
3-OST-3	GlcNAc-GlcA-GlcNS-Ido2S-**GlcNS**-Ido2S-GlcNS-GlcA-pNP	PAP	6XL8	2.34	(Wander et al., 2021)
	GlcNAc6S-GlcA-GlcNS6S-Ido2S-**GlcNS6S**-Ido2S-GlcNS6S-GlcA-pNP	PAP	6XKG	1.55	(Wander et al., 2021)
	δUA2S-IdoA2S-**GlcNS6S**-IdoA2S	PAP	1T8U	1.95	(Moon et al., 2004)
	—	PAP	1T8T	1.85	(Moon et al., 2004)
3-OST-5	—	PAP	3BD9	2.3	(Xu et al., 2008)

[a]In PDB under SULT1C1.
[b]In PDB under SULT1C2.
[c]*Gallus gallus.*
[d]*Danio rerio.*
[e]*Mus musculus.*
[f]TBP (To be published).
[g]dehydroepiandrosterone.
[h]acceptor saccharide is in bold.

acceptor substrate (Pedersen et al., 2002). Once the acceptor substrate is bound, the lysine was proposed to undergo a conformational change to hydrogen bond with the phospho-sulfo bridging oxygen, functioning as a catalytic acid to encourage dissociation of the PAP leaving group. For the SULTs, a conserved histidine was identified within hydrogen bonding distance of the acceptor hydroxyl position that could function as a catalytic base to deprotonate the acceptor group (Fig. 2B, Fig. 3, A–C) (Kakuta et al., 1997). Mutations of the conserved His108, Lys48, and Ser138 in mSULT1E1 all greatly reduced or eliminated detectable activity, supporting the proposed mechanism (Kakuta et al., 1998b; Pedersen et al., 2002).

One year after solving the structure of mSULT1E1, the Negishi laboratory solved the structure of the sulfotransferase domain (NST-1) of the bifunctional enzyme N-deacetylase/N-sulfotransferase isoform 1 (NDST-1) (Kakuta et al., 1999). This structure confirmed that conservation of the PAPS binding core for the sulfotransferases exists outside of the SULTs, including the lysine from the PSB-loop and the arginine and serine from the 3′PB motif, but lacking the conserved proposed histidine base (Fig. 2C) (Kakuta et al., 1999). The proposed catalytic histidine was later found to be conserved in Golgi HS 2-O-sulfotransferase (2-OST) and the 6-OST-1, but not in NDST-1, the 3-OSTs, or the TPSTs (Fig. 2, B–C) (Kakuta et al., 1999; Edavettal et al., 2004; Moon

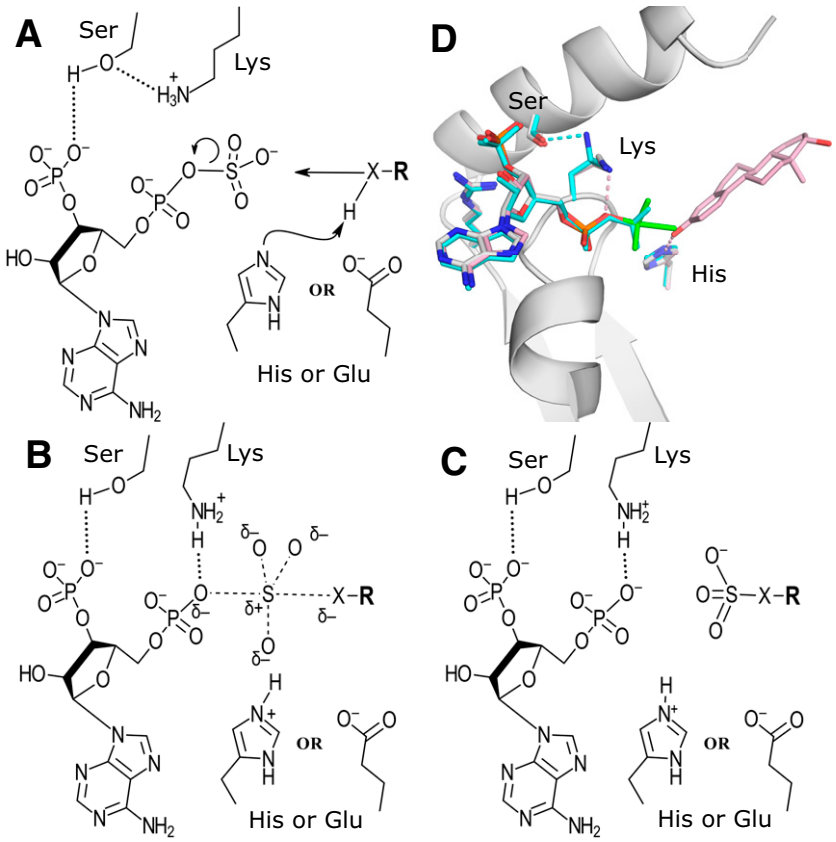

Fig. 3. Catalytic mechanism of the sulfotransferases. (A–C) Proposed catalytic mechanism of the PAPS-dependent sulfotransferases. (D) Common architecture of the sulfotransferase PAPS binding site including the PSB-loop and 3′SB strand-loop-helix from the crystal structure of mSULT1E1 (PDB code 1BO6) with PAP (white) and a vanadate molecule (green) in a trigonal bipyramidal arrangement thought to mimic the transition state. Also shown are the proposed catalytic base (His) and acid (Lys) (Kakuta et al., 1998b). Superimposed onto this structure are PAPS (cyan) and estradiol (pink) from two different structures of human SULT1E1 (PDB codes 1HY3 and 4JVL, respectively) with their equivalent His and Lys residues (Pedersen et al., 2002; Gosavi et al., 2013). When PAPS is present, the lysine forms a hydrogen bond with a conserved serine from the 3′SB binding region but is bound to the 5′-phosphate when PAP is present. These structures, combined with comparisons to uridylate kinase, shaped the hypothesis for the reaction mechanism shown in panels (A–C).

et al., 2004, 2012; Bethea et al., 2008; Xu et al., 2008, 2017b; Teramoto et al., 2013; Liu et al., 2014; Tanaka et al., 2017). In place of the histidine, these enzymes have a glutamate emanating from nonconserved structural elements within hydrogen bonding distance of the acceptor amine and hydroxyl atoms, respectively (Fig. 2C) (Kakuta et al., 1999; Edavettal et al., 2004; Moon et al., 2004, 2012; Xu et al., 2008; Teramoto et al., 2013; Tanaka et al., 2017). Mutations of these proposed alternative catalytic base residues also greatly reduced activity (Kakuta et al., 2003; Edavettal et al., 2004; Teramoto et al., 2013; Xu et al., 2017b). Noteworthy is the fact that, although the base may differ between different members of the phylogenetic family tree, the relative orientations of the acceptor to the leaving group PAP are highly conserved, supporting an inline transfer mechanism.

Interestingly, analysis using kinetic isotope effects and linear free-energy relationships on the SULTs suggests a mostly dissociative S_N1-like reaction mechanism (Chapman et al., 2003; Hoff et al., 2006). This conclusion is supported by recent crystallographic analysis of the mouse SULT2A8 (Teramoto et al., 2021). This enzyme sulfates the 7α position of bile acids. In this structure, the catalytic histidine is replaced with a leucine. Mutations to nonconserved His48 and Glu237, within proximity to the acceptor 7α-OH, show a greater impact on K_M rather than V_{max}, indicating greater importance in binding than catalysis. These results suggest in sulfotransferases that the proposed catalytic base is required less for catalysis and more for binding and likely proper positioning. It is plausible that the ratio of dissociative to associative behavior of the sulfotransferases may vary within the family.

The SULTs are believed to employ a sequential mechanism, whereby binding of both substrates occurs prior to product release (Leyh, 1993). Although the binding was originally thought to be through an ordered mechanism, recent more thorough analysis of the reaction, taking into account the formation of a dead-end product complexes, suggests the reaction may proceed via a random sequential mechanism (Zhang et al., 1998; Wang et al., 2014a, 2014b). These inhibitory dead-end complexes are present in many crystal structures and contain both the PAP product and the acceptor substrate bound (Table 1). The catalytic mechanism for SULT2A1 has been eloquently described to contain eight enzyme forms and 22 rate constants (Wang et al., 2014a). Their highly conserved sequence and structural features suggest this mechanism is maintained for many SULTs. Although the reaction may proceed regardless of which substrate binds first, positive or negative cooperativity may regulate substrate binding, suggesting a quasi-ordered mechanism may be a better description for some SULTs, depending on the enzyme and substrates examined (Tibbs et al., 2015). One example of this has been reported for SULT2A1 (Cook et al., 2012). Although SULT2A1 in the presence or absence of PAP does not demonstrate cooperative binding with dehyroepiandrosterone, it does display negative cooperativity for Raloxifene in the presence of PAP (Cook et al., 2012). This has been suggested to be due to conformational changes associated with nucleotide binding to the SULT that restricts access of larger substrates such as Raloxifene to the acceptor binding site after PAPS binds. Thus, cellular levels of PAPS may contribute to a dynamic specificity of the enzyme (Tibbs et al., 2015).

Although sharing the inline transfer geometry with the SULTs, an ordered mechanism as opposed to a bi-bi reaction mechanism has also been suggested for 6-OST-3, based on lack of binding to a substrate *N*-sulfoheparosan in the absence of PAPS (Sterner et al., 2014). Interestingly, based on liquid chromatography mass spectrometry analysis, TPSTs were originally suggested to proceed through a two-site ping-pong reaction mechanism, whereby the PAPS and substrate bind independently, and the reaction involves a covalent sulfo-histidine intermediate of the sulfotransferase prior to transfer of the sulfo group to the acceptor tyrosine substrate residue (Danan et al., 2010). However, structural comparisons of the TPST-2 ternary complex structure with bound PAP and substrate peptide to those of the SULTs and HSSTs, along with the lack of a histidine proximal to the active site, support an inline transfer. Additionally, like the 6-OST-3, PAPS/PAP was required for binding of protein to peptide column, suggesting an ordered sequential mechanism of substrate binding (Niehrs and Huttner, 1990).

Substrate Specificity of SULTs. Although the SULTs, TPSTs and HSSTs all show conservation in nucleotide binding and catalytic mechanism, they can vary greatly in acceptor substrate recognition, due to the wide ranges in shape, size, and charge of substrates. The acceptor substrates of sulfotransferases can range in size from small phenolic compounds to very large protein or proteoglycan substrates. Modes of recognition and substrate orientation inside the binding pocket can also vary within the families themselves. Due to the smaller, often hydrophobic nature of the substrates, the SULTs' acceptor substrate binding pockets are typically buried within the core of the protein by three loops (Fig. 4A) (Tibbs et al., 2015). Originally termed phenol sulfotransferases, the human SULT1 family possess a substrate gate consisting of aromatic residues (Phe80 and Phe141 in hSULT1E1) with the one exception being SULT1B1, which contains a methionine at the first position (figure 7 in Tibbs et al., 2015). These residues lie above and below the aromatic plane of the substrate and select for a phenolic acceptor, yet the rest of the pocket can accommodate diverse structural features (Fig. 4A) (Petrotchenko et al., 1999; Duffel, 2010 updated 2016). The SULT2 family were originally referred to as hydroxysteroid or bile acid sulfotransferases, but were later reclassified with the more general term alcohol sulfotransferases due to the developing knowledge of their broad specificity (Lyon and Jakoby, 1980; Duffel, 2010 updated 2016). The residues at the substrate gate differ in the SULT2 family, allowing for nonaromatic acceptors such as dehydroepiandrosterone. A thorough analysis on specificity overlap among and within the SULTs has been previously reviewed in fine detail (Duffel, 2010 updated 2016; Dong et al., 2012; Coughtrie, 2016). In general, the acceptor specificity is largely determined by three loops with variable sequences that define and restrict the entrance to the substrate binding pocket. These loops are flexible and often disordered in SULT structures, particularly in the absence of substrate (Tibbs et al., 2015). In human SULTs, loop 1 is ~9–10 residues and highly variable in the SULT1 family and is 5–6 residues shorter in the SULT2 and SULT4 families (Dong et al., 2012; Tibbs et al., 2015). It has been postulated that a smaller loop 1 for the

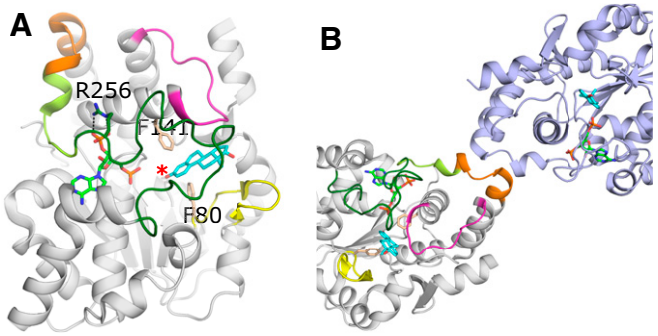

Fig. 4. Substrate binding and dimerization of SULTS. (A) A representative SULT crystal structure, SULT1E1 with PAP (green) and estradiol (cyan) bound (PDB code 4JVL) (Gosavi et al., 2013). Shown are Loops 1 (yellow), 2 (magenta), and 3 (green) that contribute to substrate specificity and binding. The SULT-specific GXXGXXK region that connects loop 3 to the dimerization domain (orange) is colored lemon. The acceptor hydroxyl of the estradiol is designated with a red asterisk. Also shown are highly conserved aromatic residues (wheat) found in the SULT1 enzymes that contribute to selectivity for phenolic compounds. (B) Dimer of SULT1E1. The dimerization domain consists of a small seven residue motif (264-270 in SULT1E1, orange) that is conserved in human SULTs. The other protomer in the dimer is shown in light purple.

SULT2s allows the binding of larger substrates compared with SULT1 family members (Dong et al., 2012). Loop 2 is located after the SB-helix and can contribute to substrate interactions (Fig. 4A). Loop 3, also referred to as "lid" or "cap", is the largest of the loops and covers both the PAPS and acceptor substrate binding sites when substrates are bound and may regulate binding cooperativity for certain substrates such as Raloxifene to SULT2A1, as mentioned previously (Cook et al., 2012; Leyh et al., 2013). Ordering of loop 3 is due in part to PAPS binding, as the conserved GXXGXXK is located at the C-terminus of this loop and, along with the preceding conserved arginine, forms interactions with the 3′-phosphate of the PAPS (Fig. 4A). In fact, there are relatively few crystal structures of sulfotransferases without nucleotides present. Binding of the nucleotide generally improves the thermostability and increases the likelihood of crystallization by decreasing surface heterogeneity via limiting loop 3 flexibility (Tibbs et al., 2015).

Single amino acid differences between isoforms SULT1A1 and SULT1A2 as well as SULT1A1 and SULT1A3 have been suggested to dictate specificity among these isoforms (Dajani et al., 1998; Lu et al., 2010; Dong et al., 2012). As well, loops 1–3 display structural plasticity within single isoforms to accommodate different acceptor substrates, accentuating the need for structures with multiple acceptors bound to better interrogate these enzymes for design of specific inhibitors (Dong et al., 2012).

Crystal structures of human SULTs revealed a conserved KXXX-TVXXXE dimerization motif that presents an unusually small protomer interface (Fig. 4B) (Petrotchenko et al., 2001; Weitzner et al., 2009). The N-terminal lysine of this motif overlaps with the C-terminal lysine of the GXXGXXK sequence involved in 3′-phosphate binding at the end of loop 3 (Fig. 4). The dimerization motif is located distal from the acceptor binding site and appears important for enzyme stability, based on studies with SULT1A1 and 1B1, but may also regulate function (Lu et al., 2009; Tibbs and Falany, 2016). Half-site reactivity has been demonstrated for SULT1E1, SULT1A1, and SULT2A1, suggesting that substrate binding at one active site may influence binding to the other protomer (Sun and Leyh, 2010; Wang et al., 2014a, 2014b). The proximity of the dimerization domain to residues involved in PAP binding suggests a potential mode of regulation described in detail by Tibbs et al. (2015). However, this theme may not be universal, as SULT1B1 forms homodimers but does not display half-site reactivity (Tibbs and Falany, 2016). Homo- and heterodimers of SULTs have been described *in vivo* (Heroux and Roth, 1988; Kiehlbauch et al., 1995). Heterodimers could provide a mechanism by which substrates of one SULT could affect sulfation of another. Also, SULT4A1 alone has been hypothesized to play important roles in neuronal development by heterodimerizing with and regulating the activity of other SULTs (Idris et al., 2020).

Substrate Specificity of TPSTs. The TPSTs have broad, overlapping substrate specificities and are believed to sulfate up to 1% of all tyrosine residues in the eukaryotic proteome (Baeuerle and Huttner, 1985; Hille et al., 1990). The human TPSTs -1 and -2 bind to intrinsically disordered sequences containing a tyrosine flanked by acidic residues within five amino acids on both the N- and C- terminal sides (Hortin et al., 1986; Rosenquist and Nicholas, 1993; Teramoto et al., 2013). The crystal structures of the catalytic domains of TPST-1 and -2 reveal that the tyrosine acceptor is buried deep within a positively charged binding pocket, necessitating the peptide to take on an intrinsically unfolded conformation (Fig. 5A) (Teramoto et al., 2013; Tanaka et al., 2017). The peptide adopts a sharply bent configuration with the bend's apex immediately N-terminal (-1 position) to the tyrosine acceptor (0 position). For TPST-1 binding to a substrate peptide, the tyrosine and aspartate at the -1 position appear to be the most critical residues for binding (Fig. 5A) (Tanaka et al., 2017). Like the human SULTs, the TPSTs form functional dimers; however, the dimerization interface is very different. For TPSTs, the dimerization interface buries ∼25% of the surface area and is located at the acceptor substrate binding pocket (Fig. 5) (Teramoto et al., 2013; Tanaka et al., 2017). Although not critical for catalysis, dimerization appears to have a role in substrate binding (Teramoto et al., 2013). Structurally located at the position of loop 1 in the SULTs are three helices that form the majority of the dimer interface (Fig. 5B). Heterodimers between TPST-1 and -2 have been reported *in vivo*, likely due to the high sequence conservation of this region (Hartmann-Fatu et al., 2015). This region also contributes to acceptor substrate binding interactions at each active site. Two conserved arginines (Arg102 and Arg106) from the first α-helix, shown to be important for binding in TPST2, interact with the substrate in the same protomer binding site, although Arg123 (not critical for catalysis from the other protomer) also simultaneously interacts with the substrate (Fig. 5A) (Teramoto et al., 2013). SULT-equivalent loop 2 from TPST forms β-sheet like interactions with the substrate peptide when present and is disordered in the absence of acceptor substrate (Teramoto et al., 2013). Although the extent of the conformational flexibility of "loop 3" in TPST remains unknown, it appears to be involved in dimer formation, exclusion of water from the active site, and PAPS binding via a serine residue that interacts with the 5′- phosphate (Fig. 5A) (Teramoto et al., 2013). It has been suggested that the presence of PAPS enhances peptide binding by organizing the substrate binding site (Niehrs and Huttner, 1990). The ability to bind and sulfonate a variety of peptide sequences may also make the enzyme susceptible to nonproductive binding, as demonstrated in the crystal structure of TPST-1, where the Gastrin peptide is interpreted to be present in both a productive and a nonproductive binding orientation (Tanaka et al., 2017).

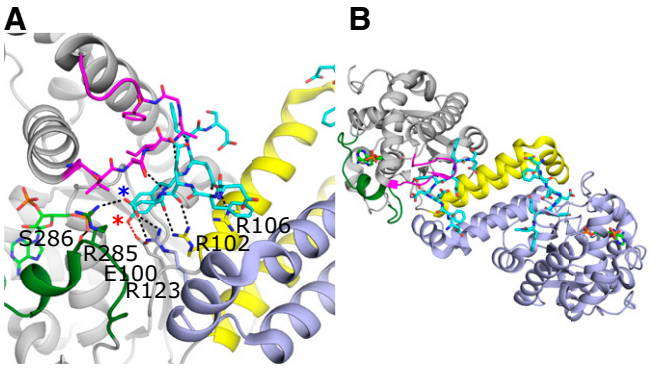

Fig. 5. Substrate binding and dimerization of TPST-1. (A) Substrate binding site of TPST-1 (PDB code 5WRI) (Tanaka et al., 2017). Residues Arg102 and Arg106 from the α-helix bundle and loop 2 (magenta) contribute significantly to substrate binding. Residues from loop 3 (green) form interactions with both the acceptor (Arg285) and donor substrates (Ser286). Arg123 from the other protomer forms a nonessential interaction with the substrate. The acceptor tyrosine is positioned for catalysis and forms a hydrogen bond with the proposed catalytic base Glu100 (red dashed line). The acceptor hydroxyl on the tyrosine and the Asp at the -1 position of the substrate are designated with red and blue asterisks, respectively. (B) Dimer interface of TPST-1. One protomer is colored light purple, whereas the other is colored gray with the equivalent to loops 1, 2, and 3 of the SULTs colored in yellow, magenta, and dark green, respectively.

Substrate Specificity of HSSTs. HSSTs are highly specific for which functional group becomes sulfated and on the types of modifications (sulfation or epimerization) on the HS that can be accommodated within the active site. Unlike the SULTs and TPSTs, these enzymes use an open binding cleft to bind the large, often anionic polysaccharide acceptor substrates. Historically, the study of these enzymes was hindered by the inability to obtain homogeneous substrates. However, with the advent of chemoenzymatic synthesis, which utilizes glycosyltransferase and sulfotransferase enzymes to produce homogenous HS with specific lengths, sequences, sulfation, and epimerization modifications,

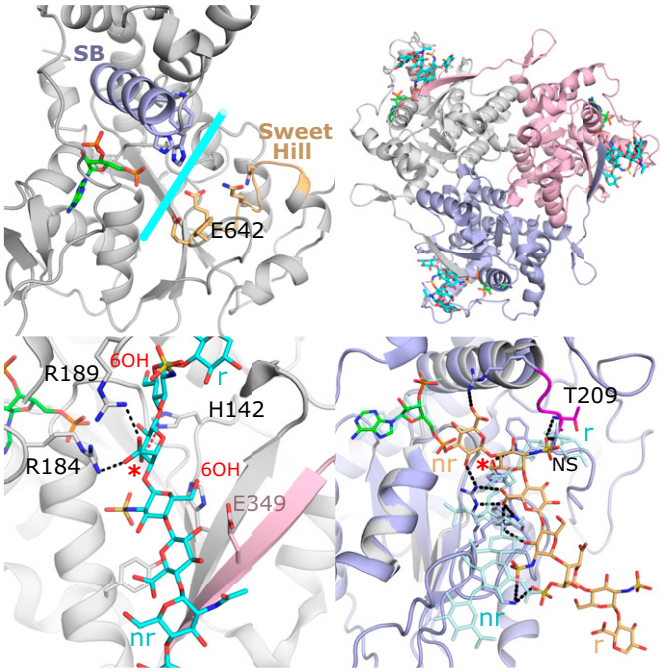

Fig. 6. Substrate binding of the heparan sulfate sulfotransferases. (A) Crystal structure of the sulfotransferase domain of NDST-1 (PDB code 1NST) with PAP shown (Kakuta et al., 1999). The regions colored in light purple (α-helix from 3′SB motif) and wheat ("Sweet Hill" region, including Glu642, the catalytic base) have been shown to be important for substrate binding and lie along an open cleft across the active site, which is similar to that seen in 3-OST-3 (Fig. 2A). (B) Crystal structure of the 2-OST trimer with protomers shown in white, light purple, and pink (PDB code 4NZD). PAP and the octasaccharide substrate bound to each active site are shown in green and cyan, respectively. Of note, the C-terminal residues of one protomer extend into the active site of the other (Liu et al., 2014). (C) Active site of 2-OST suggests how the enzyme accommodates both IdoA and GlcA in the active site by supporting binding of a $^4C_1$ acceptor sugar conformation that relies on Arg189. The positions of the 6-OH as shown would likely exclude 6S moieties, due to steric conflict on the reducing end and possible electrostatic repulsion with Glu349 from another protomer on the GlcNS on the nonreducing side. The acceptor hydroxyl of the octasaccharide is designated with a red asterisk, whereas the reducing and nonreducing ends are labeled r and nr, respectively. (D) Crystal structure of zf6-OST-3 (PDB code 5T0A) active site (light purple) with PAP (green) and bound heptamer (wheat) substrate (Xu et al., 2017b). Hydrogen bonds with substrate are shown in black dashed lines. The acceptor hydroxyl is designated with a red asterisk. 2-OST (gray) is superimposed with its substrate (transparent cyan). The superposition reveals 6-OST binds its substrate with opposite polarity, relative to the active site, as compared to 2-OST and 3-OSTs. In 6-OST, a loop including Thr209 (magenta) blocks the cleft found in the other heparan sulfotransferases and forms interactions with the *N*-sulfo moiety on the acceptor glucosamine.

cocrystal structures with acceptor substrates bound with chicken 2-OST, zebrafish 6-OST-3, and 3-OST-1 and -3 (mouse and human, respectively) have been obtained (Moon et al., 2004, 2012; Liu et al., 2014; Xu et al., 2017b; Wander et al., 2021). This structural information has provided a wealth of information into features dictating the specificity between families and isoforms within families.

Despite lacking an acceptor substrate, the crystal structure of the sulfotransferase domain of NDST-1 (NST-1) revealed a large open cleft that extends across the PAPS binding site to accommodate the acceptor substrate binding (Fig. 6A) (Kakuta et al., 1999). The NDSTs' sulfotransferase domains are most similar to that of the 3-OSTs (discussed later), with NST-1 sharing 28% sequence identity in the catalytic domain (Edavettal et al., 2004; Moon et al., 2004; Xu et al., 2008). Comparing NST-1 to the crystal structure of 3-OST-1 revealed the acceptor binding cleft to be less positively charged than that of the 3-OST-1, consistent with its substrate containing a reduced anionic charge due to its role earlier in the HS maturation process (Edavettal et al., 2004). To determine residues involved in substrate binding, an acceptor substrate was modeled into the active site (Kakuta et al., 2003). Mutations were then made to residues lining the cleft on the 3′SB helix as well as a loop coined "sweet hill", with a unique insert of residues (640–649) on the opposite side of the cleft. Residues from this motif, including the proposed catalytic base Glu642, were shown to be important for activity (Kakuta et al., 2003).

The product of the *N*-deacetylase/*N*-sulfotransferase and C_5-epimerization becomes the substrate for 2-OST. To obtain the crystal structure of chicken 2-OST (92% sequence identity to human), 2-OST was crystallized as an maltose binding protein fusion to enhance solubility and likelihood of crystallization (Bethea et al., 2008). Unlike the other HSSTs that appear to function as monomers, the structure revealed that 2-OST exists as a homotrimer with ∼24% of each protomer's surface area buried at the interface with the C-terminus of one molecule contributing to the substrate binding pocket of the other (Fig. 6, B–C). Removal of this tail disrupts trimer formation and greatly diminishes activity, supporting an important role for trimerization (Bethea et al., 2008). The active sites of each protomer are located ∼50 Å apart and are believed to function independently of one another (Liu et al., 2014). The structure revealed extensive interactions with five saccharides in the bound heptasaccharide substrate. The *N*-sulfo groups on the GlcNSs flanking the acceptor uronic acid form multiple interactions, suggesting a GlcNS-containing pentasaccharide represents the minimum binding motif required for activity (Liu et al., 2014). The structure also revealed that sulfation on the 6-OH of the adjacent GlcNS on the reducing end would result in significant steric clashes, whereas 6S on the nonreducing side could create electrostatic repulsion with the Glu349 on the neighboring protomer (Fig. 6C). Taken together, the structures support the central dogma that 2-*O*-sulfation occurs after *N*-sulfation and before 6-*O*-sulfation. Although 2-OST can transfer the sulfo group to both GlcA and IdoA saccharides, in a heptascaccharide with a mixture of GlcA or IdoA flanked by GlcNS, IdoA2S was produced 10:1 over GlcA2S (Liu et al., 2014). IdoA is typically found in $^1C_4$ or $^2S_0$, whereas GlcA adopts the $^4C_1$ conformation, suggesting that each would need to bind differently to the active site. However, the crystal structure, combined with mutagenesis, revealed that Arg189 may act to stabilize IdoA in the unexpected $^4C_1$ conformation, allowing both IdoA and GlcA to use the same active site in similar conformations (Fig. 6C) (Liu et al., 2014). In contrast, a recent molecular modeling study suggests that for longer endogenous substrates, the IdoA would be in the preferred $^1C_4$ conformation and that Arg189 sterically excludes GlcA, generating the preference for IdoA substrate (Gesteira et al., 2021).

Like 2-OST, the zebrafish 6-OST isoform 3 (zf6-OST-3; > 70% sequence identity to human isoforms) was crystallized as a maltose binding protein fusion (Xu et al., 2017b). Three crystal structures were obtained with three oligosaccharides (a hepta- and two hexasaccarides) comprised of different sequences that bound in similar conformations. Although the 6-OSTs share many features with the other HSSTs, the orientation of substrate binding is completely different, with the substrate oriented almost perpendicular to that observed in the 2-OST and 3-OST crystal structures (Fig. 6D). In all three 6-OST structures, the nonreducing end GlcNS is positioned with the 6-hydroxyl in the catalytic position. The structures revealed that the reducing end of the 2-OST and 3-OST cleft is occluded by the loop immediately after the 3′SB helix, structurally equivalent to that of loop 2 in the SULTs (Fig. 6D). The 6-OSTs are the most promiscuous of the HSSTs with 6-OST-1 requiring only a trisaccharide composed of two glucosamines (GlcNS or GlcNAc) and a central uronic acid (GlcA, IdoA, or IdoA2S) (Liu and Liu, 2011). The lack of specificity is explained by the crystal structure, which shows that the majority of the interactions are with the

acceptor GlcNS and the -GlcA-GlcNS- on its reducing side (Xu et al., 2017b). The NS on the acceptor GlcNS forms multiple interactions with the occluding "loop 2," consistent with the preference of GlcNS substrate over GlcNAc. The lack of strict specificity by these enzymes may be important to generate a larger pool of diverse HS. 6-OSTs are capable of sulfating on adjacent GlcNS-GlcA/IdoAS repeat sequences. Although all the substrates in the crystal structures bind across the reducing end of the binding interface, one of the substrates has an additional GlcA on the nonreducing side of the acceptor GlcNS, suggesting the path of the nonreducing end, if it were present, would extend across the PAPS binding site (Fig. 6D).

Humans have three isoforms of 6-OST, and the extent of specificity differences between them has been up for debate (Habuchi et al., 2000). Mapping the conserved residues of the three human isoforms onto the zf6-OST-3 revealed that all residues interacting with the substrate were conserved. This, combined with recent results of activity between the isoforms on different homogeneous substrates, supports similar specificities between the isoforms (Xu et al., 2017b).

The 3-OSTs appear to have the strictest specificity requirements of all the HSSTs (Shworak et al., 1999; Liu and Pedersen, 2007). Of the seven human isoforms, the specificity of three (3-OST-1, 3-OST-3, and 3-OST-5) have been well characterized and examined structurally (Xu et al., 2008; Moon et al., 2004, 2012; Wander et al., 2021). 3-OST-1 is responsible for producing the pentasaccharide sequence GlcNS6S-GlcA-GlcNS6S**3S**-IdoA2S-GlcNS6S with strong anticoagulant activity (Liu et al., 1996; Liu and Pedersen, 2007). Alternatively, 3-OST-3 is involved in the production of the HS co-entry receptor for HSV-1, with the petasaccharide sequence GlcNS6S-IdoA2S-GlcNS6S**3S**-IdoA2S-GlcNS6S (Shukla et al., 1999). 3-OST-5 is more promiscuous and can generate both substrates (Xia et al., 2002). Crystal structures exist for all three of these enzymes in binary complexes with PAP, and acceptor substrate-bound structures exist for 3-OST-1 and 3-OST-3 (Edavettal et al., 2004; Moon et al., 2004, 2012; Xu et al., 2008; Wander et al., 2021). Major differences in substrate specificities exist between the isoforms. 3-OST-1 prefers substrates that are 6-*O*-sulfated and contain a GlcA on the nonreducing side of the acceptor GlcNS, whereas 3-OST-3 prefers substrates lacking 6S that contain Ido2S saccharides flanking the acceptor GlcNS on both sides (Wang et al., 2017). Although substrates for both enzymes occupy the similar substrate cleft as found in NST and 2-OST, the conformations of the uronic acids differ in 3-OST-1 and -3, resulting in different interactions with the enzyme (Fig. 7A). For 3-OST-1 binding, the GlcA and IdoA2S are in the $^4C_1$ and $^1C_4$ conformation, respectively (Moon et al., 2012). For 3-OST-3, both IdoA2Ss are found in the $^2S_0$ conformation (Fig. 7A) (Wander et al., 2021). Lys259 in 3-OST-3, not conserved in 3-OST-1, along with a Na^+ ion binding site on the reducing side have been suggested to contribute to 3-OST-3 specificity (Fig. 7A) (Moon et al., 2004; Wander et al., 2021). In addition, Lys259 may help to alleviate charge repulsions between the sulfo group of the Ido2S and the carboxylate group of the Ido2S on the nonreducing and reducing sides of the acceptor GlcNS, respectively. 3-OST-1 lacks these features, contributing to its inability to accommodate a IdoA2S on the nonreducing side of the acceptor.

Based on the structures, a substrate "gate" on the nonreducing side of the substrate binding cleft has been identified (Fig. 7A) (Xu et al., 2008). Having a $^4C_1$ GlcA (3-OST-1) versus a $^2S_0$ IdoA2S (3-OST-3) on the nonreducing side of the acceptor GlcNS results in a different trajectory of the oligosaccharide through the gate for each substrate, suggesting that the different sequences for the isoforms at the gate also contribute to specificity, which has been supported with mutagenesis studies (Xu et al., 2008; Wander et al., 2021).

Whereas the 6S on two of the three ordered GlcNS6S saccharides in the 3-OST-1 heptaasaccharide substrate forms interactions with the enzyme, the 6S on the acceptor glucosamine is solvent-exposed (Moon et al., 2012). Due to the decrease in activity for 3-OST-3 on 6-*O*-sulfated substrates, it was originally hypothesized that 6S would generate steric and/or electrostatic clashes while binding to 3-OST-3. However, a crystal structure at 1.55 Å with two 3-OST-3 molecules in the asymmetric unit demonstrated that a 6S-containing octasaccharide was easily accommodated and, surprisingly, could bind in the same conformation as the octasaccharide lacking 6S (Fig. 7B) (Wander et al., 2021). In contrast, the other 3-OST-3 molecule in the asymmetric unit bound the 6S-containing octasaccharide in a nonproductive manner, binding with the opposite polarity across the binding cleft (Fig. 7B, yellow molecule). The structural information led to further analysis revealing that the 6S-containing substrate bound with 10-fold higher affinity and displayed a mix of product and substrate inhibition contributing to the perceived specificity difference (Wander et al., 2021).

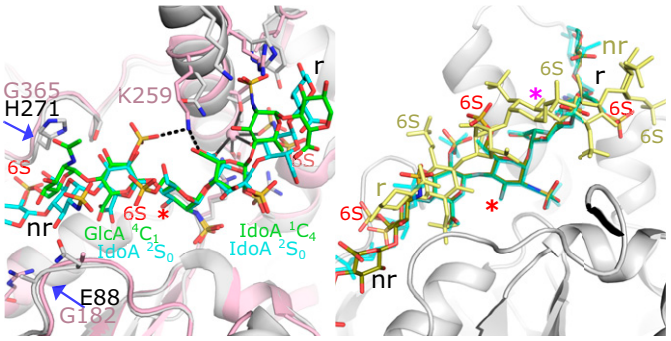

Fig. 7. Substrate binding to 3-OST-1 and 3-OST-3 active sites. (A) Crystal structure of 3-OST-3 (pink) with bound NS2S 8mer oligosaccharide (cyan) (PDB code 6XL8) superimposed with 3-OST-1 (gray) with bound heptasaccharide (green) (PDB code 3UAN) (Moon et al., 2012; Wander et al., 2021). Residue side chains that differ between the two isoforms lining the substrate binding pocket are drawn in stick. Hydrogen bonds are depicted with dashed black lines and interactions with the Na^+ ion (pink) involved in substrate binding to 3-OST-3 are shown in solid black lines. The positions of the two uronic acids flanking the acceptor glucosamine, the acceptor 3-OH on the glucosamine, and the reducing (r) and nonreducing (nr) ends of the oligosaccharide are labeled. Residues associated with the nonreducing end substrate "gate" and labeled and denoted with blue arrows. (B) Crystal structure of 3-OST-3 with the productive binding mode of NS2S6S containing 8mer bound to one protomer (olive) with the position of the NS2S6S containing 8mer in the nonproductive mode superimposed (all yellow) (PDB code 6XK6) (Wander et al., 2021). The nonproductive binding mode has reversed polarity with respect to the active site and the acceptor substrate is not in position for catalysis (magenta asterisk). The correct position for the acceptor 3OH hydroxyl is designated with a red asterisk. The NS2S substrate from the 3-OST-3 structure (PDB code 6XL8) is also superimposed (cyan) and displays very similar binding to productive positioning of the NS2S6S.

Understanding Disease through Sulfotransferase Structures. Missense genetic polymorphisms in sulfotransferases have been linked to differential metabolism of hormones and drugs by the SULTs as well as effecting activity of the HSSTs (Tornberg et al., 2011; Reuter et al., 2014; Schneeberger et al., 2020; Kurogi et al., 2021). These polymorphisms have been linked to diseases and conditions including malaria, cancer, congenital ichthyosis, idiopathic hypogonadotropic hypogonadism, and other developmental disorders including neurologic, skeletal, and renal abnormalities (Table 2). Crystal structure analysis allows for hypothesizing of how these changes may affect function. Although some of the polymorphisms are located distally from the active site and may reflect changes in the protein stability or interactions with binding partners, many of these mutations have been linked to the substrate binding loops 2 and 3 for SULTs 1A1, 1B1, 1E1, and 2B1 and could impact substrate binding and/or catalysis (Chung et al., 2009; Cohen et al., 2009; Kinnersley et al., 2016; Heinz et al., 2017). Variants associated with disease also have been found lining the substrate binding clefts of NDST-1, 2-OST, and 6-OST-1 (Najmabadi et al., 2011; Tornberg et al., 2011; Reuter et al., 2014; Schneeberger et al., 2020).

TABLE 2

Polymorphisms of human sulfotransferases with potential clinical significance

Gene	Reference SNP Cluster ID	Impact	Amino Acid Change	Location in Structure
SULT1A1	rs1042008	Increased risk of oral squamous cell carcinoma (Chung et al., 2009)	His149Tyr	Loop 2
	rs1801030	Endometrial cancer (Rebbeck et al., 2006)	Met223Val[a]	Pre-loop 3
SULT1A2	rs4987024	Inversely associated with bladder cancer risk (Figueroa et al., 2008)	Tyr62PheTyr62Cys	Away from active site
SULT1B1	rs11569729	Higher odds ratio in glioblastoma gliomas (Kinnersley et al., 2016)	Thr261Met	Loop 3
SULT1C4	Rs1402467	Increased relapse rate in acute myeloblastic leukemia (Monzo et al., 2006)	Asp5Glu[a]	N-terminus not in structure
SULT1E1		Increased risk of breast cancer (Cohen et al., 2009)	His224Gln	Pre-loop 3
SULT2B1	rs140526640	May relate to autosomal-recessive congenital ichthyosis (Youssefian et al., 2019)	Glu78Lys[a]	5′PSB-loop helix Buried H-bond to Arg100
	rs1303127476	May relate to autosomal-recessive congenital ichthyosis (Youssefian et al., 2019)	Arg100Trp[a]	Buried H-bond to Glu78
	rs1114167424	May cause autosomal-recessive congenital ichthyosis (Heinz et al., 2017)	Pro149Arg	3′SB loop
	rs1052131	Associated with esophageal squamous cell carcinoma risk (Hong et al., 2019)	Asp316Glu	C-terminus not ordered
	rs762765702	May cause autosomal-recessive ichthyosis (Heinz et al., 2017)	Arg274Gln	Loop 3, binds 3′-phosphate of PAPS
NDST1	rs606231456	Significant overlap in both demonstrated and apparent intellectual disability, muscular hypotonia, epilepsy, and postnatal growth deficiency (Najmabadi et al., 2011; Reuter et al., 2014)	Arg709Gln	On 3′SB helix
	rs606231457	Significant overlap in both demonstrated and apparent intellectual disability, muscular hypotonia, epilepsy, and postnatal growth deficiency (Reuter et al., 2014).	Glu642Asp	Catalytic base on Sweet Hill
	rs606231458	Associated with intellectual disability, muscular hypotonia, epilepsy, and postnatal growth deficiency (Reuter et al., 2014)	Phe640Leu	On Sweet Hill
	rs606231459	Associated with intellectual disability, muscular hypotonia, epilepsy, and postnatal growth deficiency (Reuter et al., 2014)	Gly611Ser	5′PSB-loop
HS2ST1[b]	rs758990524	Associated with a syndromic phenotype comprising neurologic, skeletal, and renal abnormalities (Schneeberger et al., 2020)	Asp165Tyr	3′SB loop
	rs1651972168	Associated with a syndromic phenotype comprising neurologic, skeletal, and renal abnormalities (Schneeberger et al., 2020)	Phe176Ser	3′SB helix. Lines substrate binding pocket
	rs1651973144	Associated with a syndromic phenotype comprising neurologic, skeletal, and renal abnormalities (Schneeberger et al., 2020).	Arg189Ser	Binds acceptor saccharide. Determinant residue for IdoA sulfation
HS3ST3A1	rs60532842	Associated with P. falciparum parasitaemia (Atkinson et al., 2012)	Ala85Ser	N-terminal of sulfotransferase domain
HS3ST3B1[c]	rs9906590	Associated with P. falciparum parasitaemia (Atkinson et al., 2012; Nguyen et al., 2018)	Glu363LysGlu363Gln	Away from active site
	rs62056073	Associated with P. falciparum parasitaemia (Atkinson et al., 2012; Nguyen et al., 2018)	Ile196ValIle196Phe	Away from active site
	rs62636623	Associated with P. falciparum parasitaemia (Atkinson et al., 2012; Nguyen et al., 2018)	Gly83ArgGly83Trp	N-terminal of sulfotransferase domain
HS6ST1[d]	rs780352591	Found in hypogonadotropic hypogonadism patients (Tornberg et al., 2011)	Arg306Trp[1]	Away from active site.
	rs201307896	Found in hypogonadotropic hypogonadism patients (Tornberg et al., 2011)	Arg306Gln[e]	Away from active site
	rs761325768	Found in hypogonadotropic hypogonadism patients (Tornberg et al., 2011)	Arg323Gln[e]	Lines non-reducing end of substrate binding pocket
	rs199538589	Found in hypogonadotropic hypogonadism patients (Tornberg et al., 2011; Cangiano et al., 2019; Choi et al., 2015)	Arg382Trp[e]	Extended C-terminal tail away from active site
		Found in hypogonadotropic hypogonadism patients (Tornberg et al., 2011)	Met404Val[e]	Extended C-terminal tail away from active site
HS6ST2[d]	rs866919041	Associated with X-linked intellectual disability and severe myopia in two male twins (Paganini et al., 2019).	Gly306CysGly306Arg	Disordered loop away from active site

List was obtained by utilizing the NSBI dbSNP search with clinical significance (likely pathogenic, pathogenic, and pathogenic likely pathogenic) and function class (missense).

[a]not found in NSBI dbSNP using listed criteria.

[b]HS2ST analysis based on crystal structure of chicken 2-OST PDB code 4NDZ.

[c]H3ST3B1 structural analysis based on structure of equivalent residue in H3ST3A1 PDB code 6XL8.

[d]HS6ST1 and HS6ST2 structural analysis based on crystal structure of zebrafish 6-OST-3 PDB id code 5T0A.

[e]Numbering of Arg306, Arg323, Arg382, and Met404 are listed as Arg296, Arg313, Arg372, and Met294 in Tornberg et al. (2011).

Disease-associated variants are also found clustered within the highly conserved 3′SB and 5′PSB strand-loop-helix motifs associated with PAPS and acceptor substrate binding (Reuter et al., 2014; Tibbs et al., 2018; Schneeberger et al., 2020). One of the variants for NDST-1 involves the proposed catalytic base, whereas the R189S of 2-OST involves the residue proposed to dictate specificity for IdoA over GluA (Reuter et al., 2014; Schneeberger et al., 2020). The R189S mutation would likely not inhibit GlcA binding, but would lose reactivity to IdoA, as suggested by the R189A *in vitro* studies (Liu et al., 2014).

ST Structures in Molecular Modeling. The value of sulfotransferase crystal structures has extended beyond basic understanding of the enzymatic functions, serving as a starting point for *in silico* calculations to predict substrates and inhibitors and better understand how conformational dynamics affect substrate binding. Early work applied crystal structures and homology models to an adaptation of the three-dimensional quantitative structure-activity relationship, referred to as comparative molecular field analysis, to better understand enzyme kinetics and help predict specificity of rat ASTIV and SULT1A3 (Sharma and Duffel, 2002, 2005; Sipilä et al., 2003). *In silico* docking based on crystal structures was used to determine that PAPS binding can regulate binding of larger substrates such as Raloxifene via conformational dynamics of loop 3 (Cook et al., 2012). Quantitive structure-activity relationship was later combined with molecular dynamics (MD) to consider both ligand and protein flexibility to successfully identify ligands of isoforms SULT1A1, SULT1A3, and SULT1E1 (Martiny et al., 2013). Others have used MD to study thermal stability and conformational flexibility associated with ligand binding in SULT2A1 (Zhao et al., 2015, 2016; Zhou et al., 2019; Zhu et al., 2019). Utilizing molecular dynamics and an FDA-approved small molecule drug database, Cook et al. (2013b) were able to accurately predict known substrates and identify novel substrates for SULT1A1 and SULT2A1. Further MD analysis of SULT1A1 revealed a molecular clamp by two aromatic residues that reposition to "sandwich", in a catalytically relevant position, the phenolic substrates that display enhanced affinities for binding in the presence of saturating nucleotide (Cook et al., 2015b). In contrast, substrates unaffected by nucleotide binding tend to "wander" in the binding pocket, rarely sampling a catalytically relevant position (Cook et al., 2015b). Analysis using MD simulations was also used to understand substrate inhibition differences between mouse and human SULT1E1, suggesting that a subpocket within the binding pocket of hSULT1E1 could accommodate the substrate in a noncatalytic binding mode (Stjernschantz et al., 2010). A recent approach in MD applied to SULT1A1 that includes the use of excited normal modes has been used to sample more conformational space than classic MD and may provide more insight into substrate and/or inhibitor binding (Dudas et al., 2021).

Molecular docking experiments have also been used to better understand how allosteric interactions can regulate sulfotransferase function. SULT1A1 and 1A3 have been shown to contain two allosteric binding sites (Fig. 8) (Cook et al., 2015a, 2017). Utilizing the crystal structure of SULT1A1 as a starting model of SULT1A3, monoamine neurotransmitter metabolites were screened against the known catechin-binding site of SULT1A3 predicting tetrahydrobiopterin, an essential cofactor in monoamine neurotransmitter biosynthesis, as a potential allosteric regulator of SULT1A3 activity. When tested, tetrahydrobiopterin had a K_i = 23nM for SULT1A3, but with no detectable affinity for SULT1A1, SULT1E1, SULT2A1, or SULT2B1 (Cook et al., 2017). Binding to the catechin-binding site, located at the entrance to the substrate binding pocket between loops 1 and 3, was confirmed through mutagenesis and spin-labeled triangulation NMR experiments (Cook et al., 2017). Darrah et al. (2019) identified a SULT1A3 specific inhibitor which also inhibited the sulfotransferase activity at nanomolar concentrations (K_i = ~34nM). Using spin-labeled triangulation NMR, combined with distance constraint molecular dynamics of models derived from crystal structures, a novel allosteric site specific to SULT1A3 was identified and confirmed by mutagenesis of surrounding residues (Darrah et al., 2019). This site is located outside the active site prior to loop 3, in a region disordered in the crystal structure of SULT1A3 when no substrates are present, that must open and close during catalysis to bind and release substrate (Fig. 8) (Bidwell et al., 1999; Wang et al., 2014a). A subsequent study identified two other structurally similar compounds that also inhibited with nanomolar K_is and were specific to SULT1A3 when compared with SULT1A1, SULT1E1, and SULT2A1. These compounds also inhibited SULT1A3 in cultured cells (Cook et al., 2021). Further molecular dynamics analysis supported the assessment that these compounds inhibit via loop 3 stabilization (Cook et al., 2021).

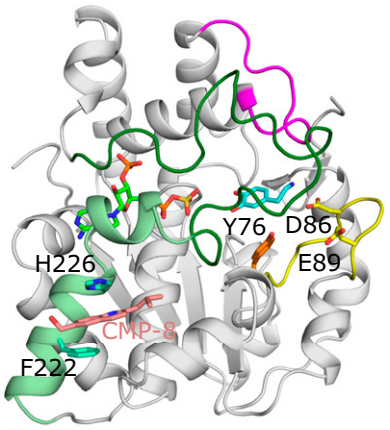

Fig. 8. The allosteric binding sites of SULT1A3. Model of SULT1A3 with bound PAPS (green) and inhibitor CMP-8 (coral) bound to an allosteric site via aromatic stacking with His226 and Phe222 (model found at: https://www.modelarchive.org/doi/10.5452/ma-qtj80) (Darrah et al., 2019). The position of the acceptor substrate dopamine (cyan) was superimposed from PDB coordinates 2A3R (Lu et al., 2005). Also shown are residues Tyr76 (orange), Asp86, and Glu89 (both yellow) that compose the catechin-binding allosteric site that binds the monoamine neurotransmitter cofactor tetrahydrobiopterin (Cook et al., 2017). Loops 1, 2, and 3 are colored yellow, magenta, and dark green, respectively, as seen in SULT1E1 (Fig. 4). In the crystal structure of SULT1A3 without substrate present, residues 216-261 are disordered. This comprises loop 3 and the two helices (light green) N-terminal to loop 3 that make up one of the allosteric binding sites (PDB code 1CJM) (Bidwell et al., 1999).

Modeling and molecular dynamics studies of HS substrates using the crystal structure of NST-1 with bound PAP has provided insight into residues that are involved in substrate recognition and influence catalysis (Gorokhov et al., 2000; Kakuta et al., 2003; Gesteira et al., 2013). Molecular dynamics was also used to provide information on global dynamics, residues involved in binding, and a possible route for HS during modification by NDST-1 and 2-OST (Gesteira and Coulson-Thomas, 2018). Conformational dynamics has also been investigated for TPST-2 (Singh et al., 2016a, 2016b).

In addition to these dynamic studies, quantum mechanics calculations as well as Quantum mechanics/molecular mechanics studies have been performed on SULT1E1, 3-OST-3, 2-OST, and 6-OST to better understand the underlying catalytic mechanisms (Bartolotti et al., 1999; Lin et al., 2006; Sousa et al., 2016; Gesteira et al., 2021). Quantum mechanics/molecular mechanics has also been applied to investigate the potential endocrine disrupting effects of hydroxylated bromodiphenyl ethers from environmental exposures via inhibition of SULT1A1 (Ma et al., 2021).

Future Directions: Utilizing Sulfotransferase Structures for the Development of New Pharmacological Tools. Crystal structures can be powerful aids in the development of novel therapeutics. The Leyh group has used structural information on the closing of loop 3 in

the presence of PAPS to design compounds that can interact with receptors but cannot be effectively sulfated by SULTs, which should increase the half-life of compounds *in vivo* (Cook et al., 2016). Such work could be useful for improved birth control bioavailability or treatment of Parkinson's disease (Cook et al., 2016). Another example is the prodrug Oxamniquine used to treat schistosomiasis, which becomes activated through sulfation by cytosolic sulfotransferases. Resistance has emerged due to sulfotransferase variants. Crystal structures of these helminth sulfotransferases are being evaluated to help design new broad-spectrum oxamniquine derivatives that kill both *S. mansoni* and *S hematobium* species (Valentim et al., 2013; Guzman et al., 2020).

Historically, the design of effective therapeutic inhibitors has been hampered by inability to obtain a high degree of specificity for individual SULTs. The recent discovery of a selective allosteric site in SULT1A3 has changed that (Cook et al., 2021). SULT1A3 is the isoform responsible for sulfating 80% of serotonin levels in the brain, resulting in decreased levels of the active neurotransmitter. Regulating unmodified serotonin levels is important for the treatment of depressive disorders. Molecular dynamics of SULT1A3 structural models, in combination with spin-labeled triangulation NMR, appears to have been critical for determining the allosteric binding pocket specific for SULT1A3. Taking advantage of ways to specifically inhibit SULT1A3 should greatly aid current and future therapeutics studies (Cook et al., 2021).

High throughput screening has recently been used to search for inhibitors of the Golgi-resident TPST and GAG sulfotransferases (Cheung et al., 2017; Byrne et al., 2018a, 2018b). Positive hits were evaluated by docking to crystal structures to validate their ability to bind to the active site (Byrne et al., 2018a, 2018b). Crystal structures of the TPSTs and HS 2-OST are also being used for structure-based design of nucleotide analog inhibitors (Kershaw et al., 2019). Such initial inhibitors could be used to improve specificity to TPSTs or 2-OST to probe function or potentially modulate disease states such as viral infection and inflammation (Byrne et al., 2018a, 2018b; Kershaw et al., 2019).

A trending method for generation of pharmacological tools to probe physiologic and pathophysiological pathways and potential therapeutics is utilization of a chemoenzymatic approach to synthesize homogeneous GAG oligosaccharides. This method makes use of recombinant glycosyltransferases and sulfotransferases to efficiently produce the desired product, in contrast to tediously purifying heterogeneous compounds from source (Xu et al., 2011, 2017a; Zhang et al., 2020). Currently this process is being used for the development of improved anticoagulant and autoinflammatory therapeutics to treat acute liver failure due to acetaminophen overdose (Xu et al., 2014, 2017a; Arnold et al., 2020; Wang et al., 2021).

Based on crystal structures of sulfotransferases engaged with oligosaccharide substrates, some of these enzymes have been engineered via site-directed mutagenesis to alter their specificities to improve control of the chemoenzymatic pathway (Xu et al., 2008, 2017b; Liu et al., 2012, 2014; Yi et al., 2020). Particularly, a triple mutation of zf6-OST-3 designed based on the crystal structures allows for sulfation only on the nonreducing terminal glucosamine, providing fine-tuned control of 6-*O*-sulfation within the chemoenzymatic synthesis pathway (Yi et al., 2020). Cytosolic sulfotransferases are also being investigated for their ability to generate sulfated products for biologic reagents and drug discovery (Lamb et al., 2006; Shi et al., 2012; Shimohira et al., 2017; Matsumura et al., 2018; Xie et al., 2020).

Historically, two obstacles to using sulfotransferases for product development were product inhibition by PAP and the cost of PAPS. Recycling PAP efficiently circumvents both obstacles by utilizing the cytosolic sulfotransferase rat ASTIV to regenerate PAPS from PAP and p-nitrophenyl sulfate (Burkart et al., 1999, 2000). In concert with production of the desired sulfated product, recycling of PAP reduces both the need for additional PAPS and reduces PAP inhibition by keeping the PAP concentration low (Burkart et al., 1999, 2000; Chen et al., 2005; Datta et al., 2020). Recent work has sought to improve upon the efficiency of this approach by re-engineering ASTIV (Zhou et al., 2019). Information obtained from the crystal structure of SULT1A1 was used to choose the loop sequence between Lys81 and Thr95 for molecular evolution that identified the double mutant L89S/E90L to have improved efficiency. These residues were then further subjected to site-saturation mutagenesis to systematically test for improved efficiency. Zhou et al. (2019) identified the variant L89M/E90Q, which has a 2-fold lower K_M and a 10-fold higher catalytic efficacy than the wild-type enzymes. This mutant could prove useful to improve chemoenzymatic synthesis by sulfotransferases. Thus, combining engineered SULTs with engineered GAG sulfotransferases could be useful in the discovery and production of pharmacological tools for probing pathways and designing therapeutics.

Conclusion

Crystal structures of the SULTs, HSSTs, and TPSTs have provided a crucial foundation of structural information to better understand the mechanisms and specificities of these enzymes. These structures are proving useful for *in silico* substrate and inhibitor screening from chemical databases as well as for inhibitor design. Mutational engineering based on the sulfotransferase structures has proven successful in altering specificity and kinetic properties. Understanding how the sulfated products of these enzymes interact with their downstream receptors and targets will likely stimulate an interactive, iterative process of redesigning the specificity of the sulfotransferases to enhance specificity of the products with their targets. The design of inhibitors along with the use of sulfotransferases in synthesizing compounds should enhance the production of pharmacological tools for probing pathways and the design of novel therapeutics.

Authorship Contributions

Performed data analysis: L.C. Pedersen, Yi.

Wrote or contributed to the writing of the manuscript: L.C. Pedersen, Yi, L.G. Pedersen, Kaminski.

Acknowledgments

The authors thank J. Krahn and L. Perera for critical reading of the manuscript and Dr. Masahiko Negishi for his mentoring and friendship as well as unwavering support of structural biology at the National Institutes of Health, National Institute of Environmental Health Sciences.

References

Alcolombri U, Elias M, and Tawfik DS (2011) Directed evolution of sulfotransferases and paraoxonases by ancestral libraries. *J Mol Biol* **411**:837–853.

Allali-Hassani A, Pan PW, Dombrovski L, Najmanovich R, Tempel W, Dong A, Loppnau P, Martin F, Thornton J, Edwards AM, et al. (2007) Structural and chemical profiling of the human cytosolic sulfotransferases. *PLoS Biol* **5**:e97.

Arnold K, Xu Y, Sparkenbaugh EM, Li M, Han X, Zhang X, Xia K, Piegore M, Zhang F, Zhang X, et al. (2020) Design of anti-inflammatory heparan sulfate to protect against acetaminophen-induced acute liver failure. *Sci Transl Med* **12**:eaav8075.

Atkinson A, Garnier S, Afridi S, Fumoux F, and Rihet P (2012) Genetic variations in genes involved in heparan sulphate biosynthesis are associated with Plasmodium falciparum parasitaemia: a familial study in Burkina Faso. *Malar J* **11**:108.

Baeuerle PA and Huttner WB (1985) Tyrosine sulfation of yolk proteins 1, 2, and 3 in Drosophila melanogaster. *J Biol Chem* **260**:6434–6439.

Bartolotti L, Kakuta Y, Pedersen L, Negishi M, and Pedersen L (1999) A quantum mechanical study of the transfer of biological sulfate. *J Mol Struc-Theochem* **461**:105–111.

Baumann E (1876) Ueber sulfosäuren im harn. *Dtsch Chem Ges*:54–58.

Beisswanger R, Corbeil D, Vannier C, Thiele C, Dohrmann U, Kellner R, Ashman K, Niehrs C, and Huttner WB (1998) Existence of distinct tyrosylprotein sulfotransferase genes: molecular characterization of tyrosylprotein sulfotransferase-2. *Proc Natl Acad Sci USA* **95**:11134–11139.

Berger I, Guttman C, Amar D, Zarivach R, and Aharoni A (2011) The molecular basis for the broad substrate specificity of human sulfotransferase 1A1. *PLoS One* **6**:e26794.

Bethea HN, Xu D, Liu J, and Pedersen LC (2008) Redirecting the substrate specificity of heparan sulfate 2-O-sulfotransferase by structurally guided mutagenesis. *Proc Natl Acad Sci USA* **105**:18724–18729.

Bettelheim FR (1954) Tyrosine-o-sulfate in a peptide from fibrinogen. *J Am Chem Soc* **76**: 2838–2839.

Bidwell LM, McManus ME, Gaedigk A, Kakuta Y, Negishi M, Pedersen L, and Martin JL (1999) Crystal structure of human catecholamine sulfotransferase. *J Mol Biol* **293**:521–530.

Bishop JR, Schuksz M, and Esko JD (2007) Heparan sulphate proteoglycans fine-tune mammalian physiology. *Nature* **446**:1030–1037.

Blanchard RL, Freimuth RR, Buck J, Weinshilboum RM, and Coughtrie MW (2004) A proposed nomenclature system for the cytosolic sulfotransferase (SULT) superfamily. *Pharmacogenetics* **14**:199–211.

Bond CS, Clements PR, Ashby SJ, Collyer CA, Harrop SJ, Hopwood JJ, and Guss JM (1997) Structure of a human lysosomal sulfatase. *Structure* **5**:277–289.

Buhl AE, Waldon DJ, Baker CA, and Johnson GA (1990) Minoxidil sulfate is the active metabolite that stimulates hair follicles. *J Invest Dermatol* **95**:553–557.

Burkart MD, Izumi M, Chapman E, Lin C-H, and Wong C-H (2000) Regeneration of PAPS for the enzymatic synthesis of sulfated oligosaccharides. *J Org Chem* **65**:5565–5574.

Burkart MD, Izumi M, and Wong CH (1999) Enzymatic regeneration of 3′-phosphoadenosine-5′-phosphosulfate using aryl sulfotransferase for the preparative enzymatic synthesis of sulfated carbohydrates. *Angew Chem Int Ed Engl* **38**:2747–2750.

Byrne DP, Li Y, Ngamlert P, Ramakrishnan K, Eyers CE, Wells C, Drewry DH, Zuercher WJ, Berry NG, Fernig DG, et al. (2018a) New tools for evaluating protein tyrosine sulfation: tyrosylprotein sulfotransferases (TPSTs) are novel targets for RAF protein kinase inhibitors. *Biochem J* **475**:2435–2455.

Byrne DP, Li Y, Ramakrishnan K, Barsukov IL, Yates EA, Eyers CE, Papy-Garcia D, Chantepie S, Pagadala V, Liu J, et al. (2018b) New tools for carbohydrate sulfation analysis: heparan sulfate 2-*O*-sulfotransferase (HS2ST) is a target for small-molecule protein kinase inhibitors. *Biochem J* **475**:2417–2433.

Cangiano B, Duminuco P, Vezzoli V, Guizzardi F, Chiodini I, Corona G, Maggi M, Persani L, and Bonomi M (2019) Evidence for a common genetic origin of classic and milder adult-onset forms of isolated hypogonadotropic hypogonadism. *J Clin Med* **8**:126.

Chang HJ, Shi R, Rehse P, and Lin SX (2004) Identifying androsterone (ADT) as a cognate substrate for human dehydroepiandrosterone sulfotransferase (DHEA-ST) important for steroid homeostasis: structure of the enzyme-ADT complex. *J Biol Chem* **279**:2689–2696.

Chapman E, Bryan MC, and Wong CH (2003) Mechanistic studies of beta-arylsulfotransferase IV. *Proc Natl Acad Sci USA* **100**:910–915.

Chatterjee B, Majumdar D, Ozbilen O, Murty CVR, and Roy AK (1987) Molecular cloning and characterization of cDNA for androgen-repressible rat liver protein, SMP-2. *J Biol Chem* **262**:822–825.

Chen J, Avci FY, Muñoz EM, McDowell LM, Chen M, Pedersen LC, Zhang L, Linhardt RJ, and Liu J (2005) Enzymatic redesigning of biologically active heparan sulfate. *J Biol Chem* **280**: 42817–42825.

Cheung ST, Miller MS, Pacoma R, Roland J, Liu J, Schumacher AM, and Hsieh-Wilson LC (2017) Discovery of a small-molecule modulator of glycosaminoglycan sulfation. *ACS Chem Biol* **12**:3126–3133.

Choi JH, Balasubramanian R, Lee PH, Shaw ND, Hall JE, Plummer L, Buck CL, Kottler ML, Jarzabek K, Wołczynski S, et al. (2015) Expanding the spectrum of founder mutations causing isolated gonadotropin-releasing hormone deficiency. *J Clin Endocrinol Metab* **100**:E1378–E1385.

Chung YT, Hsieh LL, Chen IH, Liao CT, Liou SH, Chi CW, Ueng YF, and Liu TY (2009) Sulfotransferase 1A1 haplotypes associated with oral squamous cell carcinoma susceptibility in male Taiwanese. *Carcinogenesis* **30**:286–294.

Cohen S, Laitman Y, Kaufman B, Milgrom R, Nir U, and Friedman E (2009) SULT1E1 and ID2 genes as candidates for inherited predisposition to breast and ovarian cancer in Jewish women. *Fam Cancer* **8**:135–144.

Cook I, Cacace M, Wang T, Darrah K, Deiters A, and Leyh TS (2021) Small-molecule control of neurotransmitter sulfonation. *J Biol Chem* **296**:100094.

Cook I, Wang T, Almo SC, Kim J, Falany CN, and Leyh TS (2013a) The gate that governs sulfotransferase selectivity. *Biochemistry* **52**:415–424.

Cook I, Wang T, Falany CN, and Leyh TS (2012) A nucleotide-gated molecular pore selects sulfotransferase substrates. *Biochemistry* **51**:5674–5683.

Cook I, Wang T, Falany CN, and Leyh TS (2013b) High accuracy in silico sulfotransferase models. *J Biol Chem* **288**:34494–34501.

Cook I, Wang T, Falany CN, and Leyh TS (2015a) The allosteric binding sites of sulfotransferase 1A1. *Drug Metab Dispos* **43**:418–423.

Cook I, Wang T, and Leyh TS (2015b) Sulfotransferase 1A1 substrate selectivity: a molecular clamp mechanism. *Biochemistry* **54**:6114–6122.

Cook I, Wang T, and Leyh TS (2017) Tetrahydrobiopterin regulates monoamine neurotransmitter sulfonation. *Proc Natl Acad Sci USA* **114**:E5317–E5324.

Cook I, Wang T, Wang W, Kopp F, Wu P, and Leyh TS (2016) Controlling sulfuryl-transfer biology. *Cell Chem Biol* **23**:579–586.

Coughtrie MWH (2016) Function and organization of the human cytosolic sulfotransferase (SULT) family. *Chem Biol Interact* **259** (Pt A):2–7.

Dajani R, Hood AM, and Coughtrie MWH (1998) A single amino acid, glu146, governs the substrate specificity of a human dopamine sulfotransferase, SULT1A3. *Mol Pharmacol* **54**:942–948.

Danan LM, Yu Z, Ludden PJ, Jia W, Moore KL, and Leary JA (2010) Catalytic mechanism of Golgi-resident human tyrosylprotein sulfotransferase-2: a mass spectrometry approach. *J Am Soc Mass Spectrom* **21**:1633–1642.

Darrah K, Wang T, Cook I, Cacace M, Deiters A, and Leyh TS (2019) Allosteres to regulate neurotransmitter sulfonation. *J Biol Chem* **294**:2293–2301.

Datta P, Fu L, He W, Koffas M, Dordick J and Linhardt R (2020) Expression of enzymes for 3′-phosphoadenosine-5′-phosphosulfate (PAPS) biosynthesis and their preparation for PAPS synthesis and regeneration. *Appl Microbiol Biot* **104**:7067–7078.

Dombrovski L, Dong A, Bochkarev A, and Plotnikov AN (2006) Crystal structures of human sulfotransferases SULT1B1 and SULT1C1 complexed with the cofactor product adenosine-3′-5′-diphosphate (PAP). *Proteins* **64**:1091–1094.

Dong D, Ako R, and Wu B (2012) Crystal structures of human sulfotransferases: insights into the mechanisms of action and substrate selectivity. *Expert Opin Drug Metab Toxicol* **8**:635–646.

Dudas B, Toth D, Perahia D, Nicot AB, Balog E, and Miteva MA (2021) Insights into the substrate binding mechanism of SULT1A1 through molecular dynamics with excited normal modes simulations. *Sci Rep* **11**:13129.

Duffel MW(2010 updated 2016) Sulfotransfearses, in *Comprehensive Toxicology* (McQueen CA ed) pp 367–384, Elsevier, Oxford.

Edavettal SC, Lee KA, Negishi M, Linhardt RJ, Liu J, and Pedersen LC (2004) Crystal structure and mutational analysis of heparan sulfate 3-O-sulfotransferase isoform 1. *J Biol Chem* **279**:25789–25797.

Farzan M, Mirzabekov T, Kolchinsky P, Wyatt R, Cayabyab M, Gerard NP, Gerard C, Sodroski J, and Choe H (1999) Tyrosine sulfation of the amino terminus of CCR5 facilitates HIV-1 entry. *Cell* **96**:667–676.

Figueroa JD, Malats N, García-Closas M, Real FX, Silverman D, Kogevinas M, Chanock S, Welch R, Dosemeci M, Lan Q, et al. (2008) Bladder cancer risk and genetic variation in AKR1C3 and other metabolizing genes. *Carcinogenesis* **29**:1955–1962.

Folin O and Denis W (1915) The excretion of free and conjugated phenols and phenol derivatives. *J Biol Chem* **22**:309–320.

Gamage N, Barnett A, Hempel N, Duggleby RG, Windmill KF, Martin JL, and McManus ME (2006) Human sulfotransferases and their role in chemical metabolism. *Toxicol Sci* **90**:5–22.

Gamage NU, Duggleby RG, Barnett AC, Tresillian M, Latham CF, Liyou NE, McManus ME, and Martin JL (2003) Structure of a human carcinogen-converting enzyme, SULT1A1. Structural and kinetic implications of substrate inhibition. *J Biol Chem* **278**:7655–7662.

Gamage NU, Tsvetanov S, Duggleby RG, McManus ME, and Martin JL (2005) The structure of human SULT1A1 crystallized with estradiol. An insight into active site plasticity and substrate inhibition with multi-ring substrates. *J Biol Chem* **280**:41482–41486.

Gesteira TF and Coulson-Thomas VJ (2018) Structural basis of oligosaccharide processing by glycosaminoglycan sulfotransferases. *Glycobiology* **28**:885–897.

Gesteira TF, Marforio TD, Mueller JW, Calvaresi M, and Coulson-Thomas VJ (2021) Structural determinants of substrate recognition and catalysis by heparan sulfate sulfotransferases. *ACS Catal* **11**:10974–10987.

Gesteira TF, Pol-Fachin L, Coulson-Thomas VJ, Lima MA, Verli H, and Nader HB (2013) Insights into the N-sulfation mechanism: molecular dynamics simulations of the N-sulfotransferase domain of NDST1 and mutants. *PLoS One* **8**:e70880.

Gorokhov A, Perera L, Darden TA, Negishi M, Pedersen LC, and Pedersen LG (2000) Heparan sulfate biosynthesis: a theoretical study of the initial sulfation step by N-deacetylase/N-sulfotransferase. *Biophys J* **79**:2909–2917.

Gosavi RA, Knudsen GA, Birnbaum LS, and Pedersen LC (2013) Mimicking of estradiol binding by flame retardants and their metabolites: a crystallographic analysis. *Environ Health Perspect* **121**:1194–1199.

Günal S, Hardman R, Kopriva S, and Mueller JW (2019) Sulfation pathways from red to green. *J Biol Chem* **294**:12293–12312.

Guzman M, Rugel A, Tarpley RS, Cao X, McHardy SF, LoVerde PT, and Taylor AB (2020) Molecular basis for hycanthone drug action in schistosome parasites. *Mol Biochem Parasitol* **236**:111257.

Habuchi H, Tanaka M, Habuchi O, Yoshida K, Suzuki H, Ban K, and Kimata K (2000) The occurrence of three isoforms of heparan sulfate 6-O-sulfotransferase having different specificities for hexuronic acid adjacent to the targeted N-sulfoglucosamine. *J Biol Chem* **275**:2859–2868.

Hamers T, Kamstra JH, Sonneveld E, Murk AJ, Visser TJ, Van Velzen MJ, Brouwer A, and Bergman A (2008) Biotransformation of brominated flame retardants into potentially endocrine-disrupting metabolites, with special attention to 2,2′,4,4′-tetrabromodiphenyl ether (BDE-47). *Mol Nutr Food Res* **52**:284–298.

Hartmann-Fatu C, Trusch F, Moll CN, Michin I, Hassinen A, Kellokumpu S, and Bayer P (2015) Heterodimers of tyrosylprotein sulfotransferases suggest existence of a higher organization level of transferases in the membrane of the trans-Golgi apparatus. *J Mol Biol* **427** (6 Pt B): 1404–1412.

Hashimoto Y, Orellana A, Gil G, and Hirschberg CB (1992) Molecular cloning and expression of rat liver N-heparan sulfate sulfotransferase. *J Biol Chem* **267**:15744–15750.

Heinz L, Kim GJ, Marrakchi S, Christiansen J, Turki H, Rauschendorf MA, Lathrop M, Hausser I, Zimmer AD, and Fischer J (2017) Mutations in SULT2B1 cause autosomal-recessive congenital ichthyosis in humans. *Am J Hum Genet* **100**:926–939.

Heroux JA and Roth JA (1988) Physical characterization of a monoamine-sulfating form of phenol sulfotransferase from human platelets. *Mol Pharmacol* **34**:194–199.

Hille A, Braulke T, von Figura K, and Huttner WB (1990) Occurrence of tyrosine sulfate in proteins–a balance sheet. 1. Secretory and lysosomal proteins. *Eur J Biochem* **188**:577–586.

Hoff RH, Czyryca PG, Sun M, Leyh TS, and Hengge AC (2006) Transition state of the sulfuryl transfer reaction of estrogen sulfotransferase. *J Biol Chem* **281**:30645–30649.

Hong W, Guo F, Yang M, Xu D, Zhuang Z, Niu B, Bai Q, and Li X (2019) Hydroxysteroid sulfotransferase 2B1 affects gastric epithelial function and carcinogenesis induced by a carcinogenic agent. *Lipids Health Dis* **18**:203.

Hortin G, Folz R, Gordon JI, and Strauss AW (1986) Characterization of sites of tyrosine sulfation in proteins and criteria for predicting their occurrence. *Biochem Biophys Res Commun* **141**: 326–333.

Howell WH and Holt E (1918) Two new factors in blood coagulation - heparin and pro- antithrombin. *Am J Physiol* **47**:328–341.

Idris M, Mitchell DJ, Gordon R, Sidharthan NP, Butcher NJ, and Minchin RF (2020) Interaction of the brain-selective sulfotransferase SULT4A1 with other cytosolic sulfotransferases: effects on protein expression and function. *Drug Metab Dispos* **48**:337–344.

Iozzo RV and Schaefer L (2015) Proteoglycan form and function: a comprehensive nomenclature of proteoglycans. *Matrix Biol* **42**:11–55.

Kakuta Y, Li L, Pedersen LC, Pedersen LG, and Negishi M (2003) Heparan sulphate N-sulphotransferase activity: reaction mechanism and substrate recognition. *Biochem Soc Trans* **31**: 331–334.

Kakuta Y, Pedersen LG, Carter CW, Negishi M, and Pedersen LC (1997) Crystal structure of estrogen sulphotransferase. *Nat Struct Biol* **4**:904–908.

Kakuta Y, Pedersen LG, Pedersen LC, and Negishi M (1998a) Conserved structural motifs in the sulfotransferase family. *Trends Biochem Sci* **23**:129–130.

Kakuta Y, Petrotchenko EV, Pedersen LC, and Negishi M (1998b) The sulfuryl transfer mechanism. Crystal structure of a vanadate complex of estrogen sulfotransferase and mutational analysis. *J Biol Chem* **273**:27325–27330.

Kakuta Y, Sueyoshi T, Negishi M, and Pedersen LC (1999) Crystal structure of the sulfotransferase domain of human heparan sulfate N-deacetylase/ N-sulfotransferase 1. *J Biol Chem* **274**: 10673–10676.

Kershaw NM, Byrne DP, Parsons H, Berry NG, Fernig DG, Eyers PA, and Cosstick R (2019) Structure-based design of nucleoside-derived analogues as sulfotransferase inhibitors. *RSC Advances* **9**:32165–32173.

Kester MHA, Bulduk S, Tibboel D, Meinl W, Glatt H, Falany CN, Coughtrie MWH, Bergman A, Safe SH, Kuiper GGJM, et al. (2000) Potent inhibition of estrogen sulfotransferase by hydroxylated PCB metabolites: a novel pathway explaining the estrogenic activity of PCBs. *Endocrinology* **141**:1897–1900.

Kester MHA, Bulduk S, van Toor H, Tibboel D, Meinl W, Glatt H, Falany CN, Coughtrie MWH, Schuur AG, Brouwer A, et al. (2002) Potent inhibition of estrogen sulfotransferase by hydroxylated metabolites of polyhalogenated aromatic hydrocarbons reveals alternative mechanism for estrogenic activity of endocrine disrupters. *J Clin Endocrinol Metab* **87**:1142–1150.

Khan AS, Taylor BR, Chung K, Etheredge J, Gonzales R, and Ringer DP (1993) Genomic structure of rat liver aryl sulfotransferase IV-encoding gene. *Gene* **137**:321–326.

Kiehlbauch CC, Lam YF, and Ringer DP (1995) Homodimeric and heterodimeric aryl sulfotransferases catalyze the sulfuric acid esterification of N-hydroxy-2-acetylaminofluorene. *J Biol Chem* **270**:18941–18947.

Kinnersley B, Kamatani Y, Labussière M, Wang Y, Galan P, Mokhtari K, Delattre JY, Gousias K, Schramm J, Schoemaker MJ, et al. (2016) Search for new loci and low-frequency variants influencing glioma risk by exome-array analysis. *Eur J Hum Genet* **24**:717–724.

Kurogi K, Rasool MI, Alherz FA, El Daibani AA, Bairam AF, Abunnaja MS, Yasuda S, Wilson LJ, Hui Y, and Liu MC (2021) SULT genetic polymorphisms: physiological, pharmacological and clinical implications. *Expert Opin Drug Metab Toxicol* **17**:767–784.

Lamb SS, Patel T, Koteva KP, and Wright GD (2006) Biosynthesis of sulfated glycopeptide antibiotics by using the sulfotransferase StaL. *Chem Biol* **13**:171–181.

Langford R, Hurrion E, and Dawson PA (2017) Genetics and pathophysiology of mammalian sulfate biology. *J Genet Genomics* **44**:7–20.

Lee KA, Fuda H, Lee YC, Negishi M, Strott CA, and Pedersen LC (2003) Crystal structure of human cholesterol sulfotransferase (SULT2B1b) in the presence of pregnenolone and 3′-phosphoadenosine 5′-phosphate. Rationale for specificity differences between prototypical SULT2A1 and the SULT2BG1 isoforms. *J Biol Chem* **278**:44593–44599.

Leyh TS (1993) The physical biochemistry and molecular genetics of sulfate activation. *Crit Rev Biochem Mol Biol* **28**:515–542.

Leyh TS, Cook I, and Wang T (2013) Structure, dynamics and selectivity in the sulfotransferase family. *Drug Metab Rev* **45**:423–430.

Leyte A, van Schijndel HB, Niehrs C, Huttner WB, Verbeet MP, Mertens K, and van Mourik JA (1991) Sulfation of Tyr1680 of human blood coagulation factor VIII is essential for the interaction of factor VIII with von Willebrand factor. *J Biol Chem* **266**:740–746.

Lim GB (2017) Milestone 1: discovery and purification of heparin. *Nat Rev Cardiol*.

Lin P, Yang WT, Pedersen LC, Negishi M, and Pedersen LG (2006) Searching for the minimum energy path in the sulfuryl transfer reaction catalyzed by human estrogen sulfotransferase: role of enzyme dynamics. *Int J Quantum Chem* **106**:2981–2998.

Lindahl U, Couchman J, Kimata K, and Esko JD (2015) *Proteoglycans and Sulfated Glycosaminoglycans*, Cold Spring Harbor Laboratory Press, Cold Spring Harbor, NY.

Lindahl U and Li JP (2009) Interactions between heparan sulfate and proteins-design and functional implications. *Int Rev Cell Mol Biol* **276**:105–159.

Lipmann F (1958) Biological sulfate activation and transfer. *Science* **128**:575–580.

Liu C, Sheng J, Krahn JM, Perera L, Xu Y, Hsieh PH, Dou W, Liu J, and Pedersen LC (2014) Molecular mechanism of substrate specificity for heparan sulfate 2-O-sulfotransferase. *J Biol Chem* **289**:13407–13418.

Liu J, Moon AF, Sheng J, and Pedersen LC (2012) Understanding the substrate specificity of the heparan sulfate sulfotransferases by an integrated biosynthetic and crystallographic approach. *Curr Opin Struct Biol* **22**:550–557.

Liu J and Pedersen LC (2007) Anticoagulant heparan sulfate: structural specificity and biosynthesis. *Appl Microbiol Biotechnol* **74**:263–272.

Liu J, Shworak NW, Fritze LMS, Edelberg JM, and Rosenberg RD (1996) Purification of heparan sulfate D-glucosaminyl 3-*O*-sulfotransferase. *J Biol Chem* **271**:27072–27082.

Liu R and Liu J (2011) Enzymatic placement of 6-O-sulfo groups in heparan sulfate. *Biochemistry* **50**:4382–4391.

Lu J, Li H, Zhang J, Li M, Liu MY, An X, Liu MC, and Chang W (2010) Crystal structures of SULT1A2 and SULT1A1 *3: insights into the substrate inhibition and the role of Tyr149 in SULT1A2. *Biochem Biophys Res Commun* **396**:429–434.

Lu JH, Li HT, Liu MC, Zhang JP, Li M, An XM, and Chang WR (2005) Crystal structure of human sulfotransferase SULT1A3 in complex with dopamine and 3′-phosphoadenosine 5′-phosphate. *Biochem Biophys Res Commun* **335**:417–423.

Lu LY, Chiang HP, Chen WT, and Yang YS (2009) Dimerization is responsible for the structural stability of human sulfotransferase 1A1. *Drug Metab Dispos* **37**:1083–1088.

Lu LY, Hsieh YC, Liu MY, Lin YH, Chen CJ, and Yang YS (2008) Identification and characterization of two amino acids critical for the substrate inhibition of human dehydroepiandrosterone sulfotransferase (SULT2A1). *Mol Pharmacol* **73**:660–668.

Lyle S, Stanczak J, Ng K, and Schwartz NB (1994) Rat chondrosarcoma ATP sulfurylase and adenosine 5′-phosphosulfate kinase reside on a single bifunctional protein. *Biochemistry* **33**: 5920–5925.

Lyon ES and Jakoby WB (1980) The identity of alcohol sulfotransferases with hydroxysteroid sulfotransferases. *Arch Biochem Biophys* **202**:474–481.

Ma G, Geng L, Lu Y, Wei X, and Yu H (2021) Investigating the molecular mechanism of hydroxylated bromdiphenyl ethers to inhibit the thyroid hormone sulfotransferase SULT1A1. *Chemosphere* **263**:128353.

Marsolais F and Varin L (1995) Identification of amino acid residues critical for catalysis and cosubstrate binding in the flavonol 3-sulfotransferase. *J Biol Chem* **270**:30458–30463.

Martiny VY, Carbonell P, Lagorce D, Villoutreix BO, Moroy G, and Miteva MA (2013) In silico mechanistic profiling to probe small molecule binding to sulfotransferases. *PLoS One* **8**:e73587.

Matsumura E, Nakagawa A, Tomabechi Y, Ikushiro S, Sakaki T, Katayama T, Yamamoto K, Kumagai H, Sato F, and Minami H (2018) Microbial production of novel sulphated alkaloids for drug discovery. *Sci Rep* **8**:7980.

Mishiro E, Sakakibara Y, Liu MC, and Suiko M (2006) Differential enzymatic characteristics and tissue-specific expression of human TPST-1 and TPST-2. *J Biochem* **140**:731–737.

Monzo M, Brunet S, Urbano-Ispizua A, Navarro A, Perea G, Esteve J, Artells R, Granell M, Berlanga J, Ribera JM, et al.; CETLAM (2006) Genomic polymorphisms provide prognostic information in intermediate-risk acute myeloblastic leukemia. *Blood* **107**:4871–4879.

Moon A, Edavettal SC, Krahn JX, Munoz EM, Negishi M, Linhardt RJ, Liu J, and Pedersen LC (2004) Structural analysis of the sulfotransferase (3-o-sulfotransferase isoform 3) involved in the biosynthesis of an entry receptor of herpes simplex virus 1. *J Biol Chem* **279**:45185–45193.

Moon AF, Xu Y, Woody SM, Krahn JM, Linhardt RJ, Liu J, and Pedersen LC (2012) Dissecting the substrate recognition of 3-O-sulfotransferase for the biosynthesis of anticoagulant heparin. *Proc Natl Acad Sci USA* **109**:5265–5270.

Moore KL (2003) The biology and enzymology of protein tyrosine O-sulfation. *J Biol Chem* **278**: 24243–24246.

Mueller JW, Gilligan LC, Idkowiak J, Arlt W, and Foster PA (2015) The regulation of steroid action by sulfation and desulfation. *Endocr Rev* **36**:526–563.

Müller-Dieckmann H-J and Schulz GE (1994) The structure of uridylate kinase with its substrates, showing the transition state geometry. *J Mol Biol* **236**:361–367.

Multhaupt HA and Couchman JR (2012) Heparan sulfate biosynthesis: methods for investigation of the heparanosome. *J Histochem Cytochem* **60**:908–915.

Najmabadi H, Hu H, Garshasbi M, Zemojtel T, Abedini SS, Chen W, Hosseini M, Behjati F, Haas S, Jamali P, et al. (2011) Deep sequencing reveals 50 novel genes for recessive cognitive disorders. *Nature* **478**:57–63.

Negishi M, Pedersen LG, Petrotchenko E, Shevtsov S, Gorokhov A, Kakuta Y, and Pedersen LC (2001) Structure and function of sulfotransferases. *Arch Biochem Biophys* **390**:149–157.

Nguyen NT, Vivès RR, Torres M, Delauzun V, Saesen E, Roig-Zamboni V, Lortat-Jacob H, Rihet P, and Bourne Y (2018) Genetic and enzymatic characterization of 3-O-sulfotransferase SNPs associated with Plasmodium falciparum parasitaemia. *Glycobiology* **28**:534–541.

Niehrs C and Huttner WB (1990) Purification and characterization of tyrosylprotein sulfotransferase. *EMBO J* **9**:35–42.

O'Brien PJ and Herschlag D (1998) Sulfatase activity of E-coli alkaline phosphatase demonstrates a functional link to arylsulfatases, an evolutionarily related enzyme family. *J Am Chem Soc* **120**:12369–12370.

Ouyang Yb, Lane WS, and Moore KL (1998) Tyrosylprotein sulfotransferase: purification and molecular cloning of an enzyme that catalyzes tyrosine O-sulfation, a common posttranslational modification of eukaryotic proteins. *Proc Natl Acad Sci USA* **95**:2896–2901.

Paganini L, Hadi LA, Chetta M, Rovina D, Fontana L, Colapietro P, Bonaparte E, Pezzani L, Marchisio P, Tabano SM, et al. (2019) A HS6ST2 gene variant associated with X-linked intellectual disability and severe myopia in two male twins. *Clin Genet* **95**:368–374.

Pedersen LC, Petrotchenko E, Shevtsov S, and Negishi M (2002) Crystal structure of the human estrogen sulfotransferase-PAPS complex: evidence for catalytic role of Ser137 in the sulfuryl transfer reaction. *J Biol Chem* **277**:17928–17932.

Pedersen LC, Petrotchenko EV, and Negishi M (2000) Crystal structure of SULT2A3, human hydroxysteroid sulfotransferase. *FEBS Lett* **475**:61–64.

Petrotchenko EV, Doerflein ME, Kakuta Y, Pedersen LC, and Negishi M (1999) Substrate gating confers steroid specificity to estrogen sulfotransferase. *J Biol Chem* **274**:30019–30022.

Petrotchenko EV, Pedersen LC, Borchers CH, Tomer KB, and Negishi M (2001) The dimerization motif of cytosolic sulfotransferases. *FEBS Lett* **490**:39–43.

Pica-Mattoccia L, Carlini D, Guidi A, Cimica V, Vigorosi F, and Cioli D (2006) The schistosome enzyme that activates oxamniquine has the characteristics of a sulfotransferase. *Mem Inst Oswaldo Cruz* **101** (Suppl 1):307–312.

Pouyani T and Seed B (1995) PSGL-1 recognition of P-selectin is controlled by a tyrosine sulfation consensus at the PSGL-1 amino terminus. *Cell* **83**:333–343.

Rebbeck TR, Troxel AB, Wang Y, Walker AH, Panossian S, Gallagher S, Shatalova EG, Blanchard R, Bunin G, DeMichele A, et al. (2006) Estrogen sulfation genes, hormone replacement therapy, and endometrial cancer risk. *J Natl Cancer Inst* **98**:1311–1320.

Rehse PH, Zhou M, and Lin SX (2002) Crystal structure of human dehydroepiandrosterone sulphotransferase in complex with substrate. *Biochem J* **364**:165–171.

Reuter MS, Musante L, Hu H, Diederich S, Sticht H, Ekici AB, Uebe S, Wienker TF, Bartsch O, Zechner U, et al. (2014) NDST1 missense mutations in autosomal recessive intellectual disability. *Am J Med Genet A* **164A**:2753–2763.

Robbins PW and Lipmann F (1956) Identification of enzymatically active sulfate as adenosine-3′-phosphate-5′-phosphosulfate. *J Am Chem Soc* **78**:2652–2653.

Roche P, Debellé F, Maillet F, Lerouge P, Faucher C, Truchet G, Dénarié J, and Promé J-C (1991) Molecular basis of symbiotic host specificity in Rhizobium meliloti: nodH and nodPQ genes encode the sulfation of lipo-oligosaccharide signals. *Cell* **67**:1131–1143.

Rong J, Habuchi H, Kimata K, Lindahl U, and Kusche-Gullberg M (2001) Substrate specificity of the heparan sulfate hexuronic acid 2-O-sulfotransferase. *Biochemistry* **40**:5548–5555.

Rosenquist GL and Nicholas Jr HB (1993) Analysis of sequence requirements for protein tyrosine sulfation. *Protein Sci* **2**:215–222.

Saraste M, Sibbald PR, and Wittinghofer A (1990) The P-loop–a common motif in ATP- and GTP-binding proteins. *Trends Biochem Sci* **15**:430–434.

Schneeberger PE, von Elsner L, Barker EL, Meinecke P, Marquardt I, Alawi M, Steindl K, Joset P, Rauch A, Zwijnenburg PJG, et al. (2020) Bi-allelic pathogenic variants in HS2ST1 cause a syndrome characterized by developmental delay and corpus callosum, skeletal, and renal abnormalities. *Am J Hum Genet* **107**:1044–1061.

Sharma V and Duffel MW (2002) Comparative molecular field analysis of substrates for an aryl sulfotransferase based on catalytic mechanism and protein homology modeling. *J Med Chem* **45**:5514–5522.

Sharma V and Duffel MW (2005) A comparative molecular field analysis-based approach to prediction of sulfotransferase catalytic specificity. *Methods Enzymol* **400**:249–263.

Shevtsov S, Petrotchenko EV, Pedersen LC, and Negishi M (2003) Crystallographic analysis of a hydroxylated polychlorinated biphenyl (OH-PCB) bound to the catalytic estrogen binding site of human estrogen sulfotransferase. *Environ Health Perspect* **111**:884–888.

Shi D, Sheng A, and Chi L (2021) Glycosaminoglycan-protein interactions and their roles in human disease. *Front Mol Biosci* **8**:639666.

Shi R, Munger C, Kalan L, Sulea T, Wright GD, and Cygler M (2012) Sulfonation of glycopeptide antibiotics by sulfotransferase StaL depends on conformational flexibility of aglycone scaffold. *Proc Natl Acad Sci USA* **109**:11824–11829.

Shimohira T, Kurogi K, Hashiguchi T, Liu MC, Suiko M, and Sakakibara Y (2017) Regioselective production of sulfated polyphenols using human cytosolic sulfotransferase-expressing Escherichia coli cells. *J Biosci Bioeng* **124**:84–90.

Shukla D, Liu J, Blaiklock P, Shworak NW, Bai X, Esko JD, Cohen GH, Eisenberg RJ, Rosenberg RD, and Spear PG (1999) A novel role for 3-O-sulfated heparan sulfate in herpes simplex virus 1 entry. *Cell* **99**:13–22.

Shworak NW, Liu J, Petros LM, Zhang L, Kobayashi M, Copeland NG, Jenkins NA, and Rosenberg RD (1999) Multiple isoforms of heparan sulfate D-glucosaminyl 3-O-sulfotransferase. Isolation, characterization, and expression of human cdnas and identification of distinct genomic loci. *J Biol Chem* **274**:5170–5184.

Singh W, Karabencheva-Christova TG, Black GW, Sparagano O, and Christov CZ (2016a) Conformational flexibility influences structure-function relationships in tyrosyl protein sulfotransferase-2. *RSC Advances* **6**:11344–11352.

Singh W, Karabencheva-Christova TG, Sparagano O, Black GW, Petrov PY, and Christov CZ (2016b) Dimerization and ligand binding in tyrosylprotein sulfotransferase-2 are influenced by molecular motions. *RSC Advances* **6**:18542–18548.

Sipilä J, Hood AM, Coughtrie MW, and Taskinen J (2003) CoMFA modeling of enzyme kinetics: K(m) values for sulfation of diverse phenolic substrates by human catecholamine sulfotransferase SULT1A3. *J Chem Inf Comput Sci* **43**:1563–1569.

Sousa RP, Fernandes PA, Ramos MJ, and Brás NF (2016) Insights into the reaction mechanism of 3-O-sulfotransferase through QM/MM calculations. *Phys Chem Chem Phys* **18**:11488–11496.

Sterner E, Li L, Paul P, Beaudet JM, Liu J, Linhardt RJ, and Dordick JS (2014) Assays for determining heparan sulfate and heparin O-sulfotransferase activity and specificity. *Anal Bioanal Chem* **406**:525–536.

Stjernschantz E, Reinen J, Meinl W, George BJ, Glatt H, Vermeulen NP, and Oostenbrink C (2010) Comparison of murine and human estrogen sulfotransferase inhibition in vitro and in silico–implications for differences in activity, subunit dimerization and substrate inhibition. *Mol Cell Endocrinol* **317**:127–140.

Sun M and Leyh TS (2010) The human estrogen sulfotransferase: a half-site reactive enzyme. *Biochemistry* **49**:4779–4785.

Tanaka S, Nishiyori T, Kojo H, Otsubo R, Tsuruta M, Kurogi K, Liu MC, Suiko M, Sakakibara Y and Kakuta Y (2017) Structural basis for the broad substrate specificity of the human tyrosylprotein sulfotransferase-1. *Sci Rep-Uk* **7**.

Teramoto T, Fujikawa Y, Kawaguchi Y, Kurogi K, Soejima M, Adachi R, Nakanishi Y, Mishiro-Sato E, Liu MC, Sakakibara Y, et al. (2013) Crystal structure of human tyrosylprotein sulfotransferase-2 reveals the mechanism of protein tyrosine sulfation reaction. *Nat Commun* **4**:1572.

Teramoto T, Nishio T, Kurogi K, Sakakibara Y, and Kakuta Y (2021) The crystal structure of mouse SULT2A8 reveals the mechanism of 7α-hydroxyl, bile acid sulfation. *Biochem Biophys Res Commun* **562**:15–20.

Tibbs ZE and Falany CN (2016) An engineered heterodimeric model to investigate SULT1B1 dependence on intersubunit communication. *Biochem Pharmacol* **115**:123–133.

Tibbs ZE, Guidry AL, Falany JL, Kadlubar SA, and Falany CN (2018) A high frequency missense SULT1B1 allelic variant (L145V) selectively expressed in African descendants exhibits altered kinetic properties. *Xenobiotica* **48**:79–88.

Tibbs ZE, Rohn-Glowacki KJ, Crittenden F, Guidry AL, and Falany CN (2015) Structural plasticity in the human cytosolic sulfotransferase dimer and its role in substrate selectivity and catalysis. *Drug Metab Pharmacokinet* **30**:3–20.

Tornberg J, Sykiotis GP, Keefe K, Plummer L, Hoang X, Hall JE, Quinton R, Seminara SB, Hughes V, Van Vliet G, et al. (2011) Heparan sulfate 6-O-sulfotransferase 1, a gene involved in extracellular sugar modifications, is mutated in patients with idiopathic hypogonadotrophic hypogonadism. *Proc Natl Acad Sci USA* **108**:11524–11529.

Valentim CL, Cioli D, Chevalier FD, Cao X, Taylor AB, Holloway SP, Pica-Mattoccia L, Guidi A, Basso A, Tsai IJ, et al. (2013) Genetic and molecular basis of drug resistance and species-specific drug action in schistosome parasites. *Science* **342**:1385–1389.

Wander R, Kaminski AM, Xu Y, Pagadala V, Krahn JM, Pham TQ, Liu J, and Pedersen LC (2021) Deciphering the substrate recognition mechanisms of the heparan sulfate 3-O-sulfotransferase-3. *RSC Chemical Biology* **2**:1239–1248.

Wang T, Cook I, Falany CN, and Leyh TS (2014a) Paradigms of sulfotransferase catalysis: the mechanism of SULT2A1. *J Biol Chem* **289**:26474–26480.

Wang T, Cook I, and Leyh TS (2014b) 3′-Phosphoadenosine 5′-phosphosulfate allosterically regulates sulfotransferase turnover. *Biochemistry* **53**:6893–6900.

Wang Z, Arnold K, Dhurandhare VM, Xu Y, and Liu J (2021) Investigation of the biological functions of heparan sulfate using a chemoenzymatic synthetic approach. *RSC Chem Biol* **2**:702–712.

Wang Z, Hsieh P-H, Xu Y, Thieker D, Chai EJE, Xie S, Cooley B, Woods RJ, Chi L, and Liu J (2017) Synthesis of 3-O-sulfated oligosaccharides to understand the relationship between structures and functions of heparan sulfate. *J Am Chem Soc* **139**:5249–5256.

Weinshilboum R and Otterness D (1994) Sulfotransferase Enzymes, in *Conjugation—Deconjugation Reactions in Drug Metabolism and Toxicity* (Kauffman FC ed) pp 45–78, Springer Berlin Heidelberg, Berlin, Heidelberg.

Weitzner B, Meehan T, Xu Q, and Dunbrack Jr RL (2009) An unusually small dimer interface is observed in all available crystal structures of cytosolic sulfotransferases. *Proteins* **75**:289–295.

Xia G, Chen J, Tiwari V, Ju W, Li JP, Malmstrom A, Shukla D, and Liu J (2002) Heparan sulfate 3-O-sulfotransferase isoform 5 generates both an antithrombin-binding site and an entry receptor for herpes simplex virus, type 1. *J Biol Chem* **277**:37912–37919.

Xie L, Xiao D, Wang X, Wang C, Bai J, Yue Q, Yue H, Li Y, Molnár I, Xu Y, et al. (2020) Combinatorial biosynthesis of sulfated benzenediol lactones with a phenolic sulfotransferase from fusarium graminearum PH-1. *MSphere* **5**:e00949-20.

Xu D, Moon AF, Song D, Pedersen LC, and Liu J (2008) Engineering sulfotransferases to modify heparan sulfate. *Nat Chem Biol* **4**:200–202.

Xu Y, Cai C, Chandarajoti K, Hsieh PH, Li L, Pham TQ, Sparkenbaugh EM, Sheng J, Key NS, Pawlinski R, et al. (2014) Homogeneous low-molecular-weight heparins with reversible anticoagulant activity. *Nat Chem Biol* **10**:248–250.

Xu Y, Chandarajoti K, Zhang X, Pagadala V, Dou W, Hoppensteadt DM, Sparkenbaugh EM, Cooley B, Daily S, Key NS, et al. (2017a) Synthetic oligosaccharides can replace animal-sourced low-molecular weight heparins. *Sci Transl Med* **9**:eaan5954.

Xu Y, Masuko S, Takieddin M, Xu H, Liu R, Jing J, Mousa SA, Linhardt RJ, and Liu J (2011) Chemoenzymatic synthesis of homogeneous ultralow molecular weight heparins. *Science* **334**:498–501.

Xu Y, Moon AF, Xu S, Krahn JM, Liu J, and Pedersen LC (2017b) Structure based substrate specificity analysis of heparan sulfate 6-O-sulfotransferases. *ACS Chem Biol* **12**:73–82.

Xu ZH, Otterness DM, Freimuth RR, Carlini EJ, Wood TC, Mitchell S, Moon E, Kim UJ, Xu JP, Siciliano MJ, et al. (2000) Human 3′-phosphoadenosine 5′-phosphosulfate synthetase 1 (PAPSS1) and PAPSS2: gene cloning, characterization and chromosomal localization. *Biochem Biophys Res Commun* **268**:437–444.

Yi L, Xu Y, Kaminski AM, Chang X, Pagadala V, Horton M, Su G, Wang Z, Lu G, Conley P, et al. (2020) Using engineered 6-*O*-sulfotransferase to improve the synthesis of anticoagulant heparin. *Org Biomol Chem* **18**:8094–8102.

Youssefian L, Vahidnezhad H, Saeidian AH, Touati A, Sotoudeh S, Mahmoudi H, Mansouri P, Daneshpazhooh M, Aghazadeh N, Hesari KK, et al. (2019) Autosomal recessive congenital ichthyosis: genomic landscape and phenotypic spectrum in a cohort of 125 consanguineous families. *Hum Mutat* **40**:288–298.

Zerbino DR, Achuthan P, Akanni W, Amode MR, Barrell D, Bhai J, Billis K, Cummins C, Gall A, Girón CG, et al. (2018) Ensembl 2018. *Nucleic Acids Res* **46** (D1):D754–D761.

Zhang H, Varlamova O, Vargas FM, Falany CN, and Leyh TS (1998) Sulfuryl transfer: the catalytic mechanism of human estrogen sulfotransferase. *J Biol Chem* **273**:10888–10892.

Zhang X, Lin L, Huang H, and Linhardt RJ (2020) Chemoenzymatic synthesis of glycosaminoglycans. *Acc Chem Res* **53**:335–346.

Zhao L, Zhang P, Long S, Wang L, Jin H, Han W, and Tian P (2016) Investigating the substrate binding mechanism of sulfotransferase 2A1 based on substrate tunnel analysis: a molecular dynamics simulation study. *J Mol Model* **22**:176.

Zhao L, Zhang P, Long S, Wang L, and Tian P (2015) The impact of ligands on the structure and flexibility of sulfotransferases: a molecular dynamics simulation study. *J Mol Model* **21**:190.

Zhou Z, Li Q, Xu R, Wang B, Du G and Kang Z (2019) Secretory expression of the rat aryl sulfotransferases IV with improved catalytic efficiency by molecular engineering. *3 Biotech* **9**:246.

Zhu J, Qi R, Liu Y, Zhao L, and Han W (2019) Mechanistic insights into the effect of ligands on structural stability and selectivity of sulfotransferase 2A1 (SULT2A1). *ACS Omega* **4**:22021–22034.

Address correspondence to: Lars C. Pedersen, National Institute of Environmental Health Sciences, 111 TW Alexander Drive, RTP, NC 27709. E-mail: pederse2@niehs.nih.gov